

INVESTIGATION OF THE EFFECTS OF
ANESTHETIC COMPOUNDS
ON LIPID BILAYER ORGANIZATION

By

Katherine L. Logan-Dinco

A THESIS

Submitted to
Michigan State University
in partial fulfillment of the requirements
for the degree of

Chemistry - Master Of Science

2013

ABSTRACT

INVESTIGATION OF THE EFFECTS OF ANESTHETIC COMPOUNDS ON LIPID BILAYER ORGANIZATION

By

Katherine L. Logan-Dinco

The present thinking in the scientific field about anesthetic action has evolved into two hypotheses, both of which involve the cellular plasma membrane. The investigations presented in this thesis focused on understanding interactions between model lipid bilayer structures and three general anesthetics (pentobarbital, isoflurane and halothane) to determine the effect(s) of direct interactions between bilayers and anesthetics. The synthetic vesicles used in this work were intended to mimic qualitatively the neuronal membrane in lipid composition. For spectroscopic investigations, 0.5 – mole % perylene was added to the vesicle mixture prior to vesicle formation. Fluorescence anisotropy decay measurements were used to investigate the local environment formed by the lipid bilayer acyl chain region in the vesicles. The acyl chain region of the vesicles was seen to undergo a change in the extent of the organization observed with the control when exposed to selected anesthetics. These changes were observed with the change in acyl chain viscosity. The change in local organization sensed by perylene rotational diffusion was seen to be similar for all anesthetics used despite the absence of structural similarities among the anesthetics. In all cases, a change in the organization of the lipid bilayer was seen for anesthetic concentrations of *ca.* 4 mM. In all cases, the change in lipid organization was observed to be an increase in the rate of rotational motion of perylene about the axis perpendicular to its pi-system plane.

ACKNOWLEDGEMENTS

First and for most I would like to thank God for giving me the family, mentor, friends, and guidance committee to take on such an accomplishment. Without the triumphs and struggles He has helped me through it all or I would not be here today.

Next I want to thank my advisor, Gary Blanchard, for giving me a chance to learn spectroscopy and making me care about it! I want to thank him for his guidance, patience, understanding, and most of all for his faith in me especially when I was running low. Also, Gary thank you for not letting me quit when the times got rough and for trying to learn more biology so I could feel like I fit into the group.

My committee has been wonderful to me so thank you very much Dana Spence, Greg Swain, and James Galligan. Thank you for your support in my educational growth as well as research growth. Thank you for the guidance that you have given me. A special thanks to Dana Spence for convincing me to apply to MSU and for being a friendly face that I can always ask advice from!

I would like to thank my group, Doug Gornowich, Christine Hay, Iwan Setiawan, Chen Qiu, Fredy Pratama and last but not least not only my lab mate but best friend Kimberly Bostwick. I would also like to give a special thanks to our visiting student from Poland Krzysztof Nawara. Thank you all for listening to so many presentations and for the advice you had shared. Kim, thank you for being a great inspiration to me not only as a lab mate but as a friend. I could have not done this without you girl!! You are one of the most amazing, well rounded, and balanced people I have ever met and have had the pleasure to call a friend.

Krzysztof, thank you for teaching me how to use the instruments, asking me how they work and about my research all time to insure I was getting it right; you will make an excellent teacher one day.

There were also so many people at State that helped me along the way through thick and thin that deserve special mention here: Dr. A. Dan Jones, Joni Tucker, LeighAnn Jordan, Marion France, Prabodha Ekanayaka and Cynthia Kaeser. Without them I would have been lost and would have never made it through this process and for that I am thankful!

Last but not least my most supportive network my loving family. Mom and Dad thank you for all the years teaching me the tool to be a strong independent woman. Thank you for the love, support, discipline, guidance, and forgiveness. Theron, thank you for being the best little brother in the world, for all the laughs, fights, and crazy times we have shared to get me to where I am today . . . also thank you for proof reading! I would like to thank my in-laws for their support in my studies and for my husband. Finally, I want to thank my husband, Dan, who has been the backbone for me over the last two years and my best friend for the last nine years. Thank you for the support and bearing the brunt of my emotions. I love you more than anything in the world!

TABLE OF CONTENTS

LIST OF TABLES.....	vi
LIST OF FIGURES.....	vii
LIST OF EQUATIONS.....	ix
CHAPTER 1.....	1
INTRODUCTION	
CHAPTER 2.....	28
EXPERIMENTAL PROCEDURES	
CHAPTER 3.....	36
RESULTS AND DISCUSSION	
CHAPTER 4.....	52
CONCLUSIONS	
LITERATURE CITED.....	54

LIST OF TABLES

Table 1.1: This table is a summary of the important properties of the inhaled anesthetics halothane and isoflurane. MW - molecular weight, BP - boiling point, SVP - saturated vapor pressure, MAC - minimal alveolar concentration, O/W - oil water, Bl/G - blood gas, W/G - water gas, Br/G - brain gas, O/G - oil gas, Br/Bl brain blood interfaces ^[43]27

Table 3.1: Fluorescence lifetime and anisotropy decay time constants as a function of anesthetic concentration. The fluorescence lifetime data were fitted to a single exponential decay function and the anisotropy decay data were fitted to a two-exponential decay component function.....43

Table 3.2: D_z , D_x , D_z/D_x , τ_{DSE} and η_{DSE} values derived from experimental data as a function of anesthetic concentration.44

LIST OF FIGURES

Figure 1.1: Thiopental the first IV anesthetic discovered independently in the 1950's by two separate groups.....	3
Figure 1.2: A. Albuterol has 2 stereoisomers one of which causes undesirable side effects B. Xopenex® contains the purified R isomer of albuterol.....	8
Figure 1.3: Structures of A. Sevoflurane; B. Isoflurane; C. Thioental; D. Pentobarbital; E. Nipectic.....	12
Figure 1.4: Structure of Enfurane.....	13
Figure 1.5: Propofol is a commonly used barbiturate.....	14
Figure 1.6: Refined structure of the nicotinic acetylcholine receptor at 4A resolution. Unwin, N., (2005) J.Mol.Biol.346: 967.....	15
Figure 1.7: A. DPH is a non-polar chromophore; B. TMA-DPH is polar.....	17
Figure 1.8: Structure of DPPC.....	18
Figure 1.9: Left DPPE with an NBD chromophore tag, 1,2-dioleoyl- <i>sn</i> -glycero-3-phosphoethanolamine-N-(7-nitro-2-1,3-benzoxadiazol-4-yl) (ammonium salt). Right DPPA, 1,2-dihexadecanoyl- <i>sn</i> -glycero-3-phosphate (sodium salt).....	21
Figure 1.10: Structure of Perylene.....	22
Figure 1.11: Structure of Cholesterol.....	22
Figure 1.12: Structure of Halothane.....	27
Figure 2.1: Structure of Tris - HCl ®.....	30
Figure 2.2: Representative schematic of TCSPC Instrument.....	32

Figure 2.3: Schematic of the principles behind the anisotropy decay measurement35

Figure 3.1. Left: Structure, excitation and emission spectra of perylene. Right: Structure of 18:1 NBD-PE 1,2-dioleoyl-*sn*-glycero-3-phosphoethanolamine-N-(7-nitro-2-1,3-benzoxadiazol-4-yl) (ammonium salt).....37

Figure 3.2: A. How perylene would orientate in the Cartesian components if it were a prolate rotor B. How perylene would orientate in the Cartesian components if it were an oblate rotor 41

Figure 3.3: A. How perylene would orientate in the Cartesian components if it were a prolate rotor, B. How perylene would orientate in the Cartesian components if it were an oblate rotor 45

Figure 3.4. Dependence of lipid bilayer acyl chain region viscosity, detected by rotational diffusion measurements, on the identity and concentration of anesthetic present in the vesicle containing solution.....45

Figure 3.5. Top: D_z and D_x (GHz) as a function of pentobarbital concentration. Bottom: D_z/D_x as a function of pentobarbital concentration.....47

Figure 3.6. Top: D_z and D_x (GHz) as a function of isoflurane concentration. Bottom: D_z/D_x as a function of isoflurane concentration.....48

Figure 3.7. Top: D_z and D_x (GHz) as a function of halothane concentration. Bottom: D_z/D_x as a function of halothane concentration.....49

LIST OF EQUATIONS

Equation 1.1 $A = \epsilon bc$	23
Equation 1.2 $\phi = \frac{k_r}{k_r + k_{in} + k_{ec} + k_{ic} + k_{pd} + k_d}$	23
Equation 1.3 $\frac{P}{P_0} = 10^{-\epsilon bc}$	24
Equation 1.4 $F = K' P_0 (1 - 10^{-\epsilon bc})$	25
Equation 2.1 $k = k_r + k_{nr}$	33
Equation 2.2 $\tau_{fl} = 1/k$	33
Equation 2.3 $I(t) = I(0) \exp(-t/\tau(fl))$	33
Equation 2.4 $I(\theta) = 0.5(3 \cos^2 \theta - 1)$	33
Equation 2.5 $R = \frac{I_{\parallel}(t) - I_{\perp}(t)}{I_{\parallel}(t) + 2I_{\perp}(t)}$	34
Equation 2.6 $\tau_{or} = \frac{1}{6D_{rot}} = \frac{\eta V f}{k_B T}$	35
Equation 3.1 $\tau_{or} = 6D^{-1} = \frac{\eta V}{k_B T}$	40
Equation 3.2 $R(t) = 0.4 \exp(-6D_z t)$	40
Equation 3.3 $R(t) = 0.1 \exp(-(2D_x + 4D_x)t) + 0.03 \exp(-6D_x t)$	41

Equation 3.4 $D_x = \frac{1}{6\tau_{slow}}$ 42

Equation 3.5 $D_z = \frac{1}{4} \left(\frac{1}{\tau_{fast}} - \frac{1}{3\tau_{slow}} \right)$ 42

CHAPTER 1

INTRODUCTION

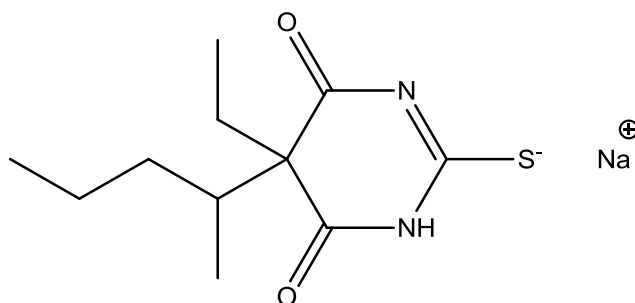
Twenty to thirty million Americans undergo surgeries with the use of general anesthetics every year for minor, major, and cosmetic surgeries.¹ Approximately 1 of every 13,000 individuals who undergo surgery dies due to complications related to anesthetic use.² These fatalities can take many forms from cardiac arrest, pulmonary arrest, and drug overdoses. All of these factors are caused by a reaction to the anesthetic being administered. While there are factors that increase an individual's risk of complications from surgery, such as obesity, smoking, heart problems, and allergies, there is still a risk of undergoing general anesthetics for surgery from the anesthetics themselves. General anesthetics are classified as organic agents that, when delivered, cause a reversible loss of consciousness (awareness of surrounding) which is defined by a combination of three states: analgesia (pain relief), amnesia (loss of memory), and immobilization.³ These agents must be administered intravenously or through inhalation. There have been many hypotheses over the last century regarding the mechanism(s) of anesthetic action. It was once believed that the anesthetic entered cells through an unknown way and caused an unknown disruption in the cell network or that anesthetics interact with regions on the neuronal cell membrane causing lateral changes in pressure that causes fluidization of the membrane⁴⁻⁶, or even that the anesthetic interacts directly with proteins in the membranes causing analgesia, amnesia, and immobilization⁷.

Acts of crude anesthesiology have been reported since 1846, when patients were given diethyl ether vapor, ethanol (to the point of intoxication), or opioids before limbs were

amputated, wounds sewn, or bullets removed from the body.⁸ Prior to the 1840's, doctors and dentists would only perform surgical procedures that were absolutely necessary to save an individual's life since the patient had to endure pain with no relief because they were conscious during the surgery.⁹ Many patients would die from bacterial infection contracted during or after surgery, due to both sanitary conditions and the use of surgery as a last resort. In 1846, a dentist, William Morton¹⁰, showed that if a cloth was soaked in diethyl ether and held to the mouth and nose of the individual, after some time the individual would appear to be in a sleeping state.⁹ There was, however, no way to control the dosage of inhaled ether fumes and the patient could either awaken during the surgical procedure or die from an anesthetic overdose. In addition to dosage issues, the storage and transportation of ether was also dangerous for reasons of flammability. Subsequent to the discovery of ether as an inhaled anesthetic, other compounds, including chloroform and nitrous oxide,¹¹ were discovered. While these compounds were also potentially dangerous in terms of dosing, they were safer to transport. The dosing of inhaled anesthetics continues to be problematic, with the attendant issues of monitoring being relegated to vital sign measurement and observation (*e.g.* heart rhythm, breathing changes, lower blood pressure, nausea, and vomiting⁹).

The development of hollow needles (1844)¹² led to the creation of syringes (1853)¹², and the intravenous (IV) drip (1930),¹³ allowing the IV introduction of anesthetics.¹¹ In 1932, the first successful barbiturate, thiopental (Figure 1.1), was introduced and was used widely as an IV anesthetic.¹⁴ Barbiturates have many disadvantages, including their depressant effect(s) on the

cardiovascular, the pulmonary, and the neurological systems. As with ether, a barbiturate overdose can cause death. Two clinical research groups reported independently the use of thiopental as an IV anesthetic,^{15,16} and this compound is still in use today. Thiopental is administered in a liquid form directly into the blood stream where it can easily cross the blood brain barrier (BBB).



(RS)-[5-ethyl-4,6-dioxo-5-(pentan-2-yl)-1,4,5,6-tetrahydropyrimidin-2-yl]sulfanide sodium

Figure 1.1: Thiopental, the first IV anesthetic discovered independently in the 1950's by two separate groups.

Current research has shown that general anesthesia produces a combination of neuropharmacological actions that are specific to each individual neuronal pathway in different regions of the central nervous system (CNS), in proportion to the dose administered.^{11,16} This means that a particular anesthetic will elicit different responses (or release of different concentrations of neurotransmitters) from different regions in the brain, these changes are dependent on the drug administered, the concentration administered, the duration of administration, as well as the individual themselves. Since the 1930's, researchers and medical professionals have determined that a titration of amnesia, analgesia, and immobility drugs over time is much safer than administering a single large bolus of anesthetic drug at the time of initial

sedation. From the onset of anesthetic administration the dose, time, and particular anesthetic administered was not an exact science because the mechanism of anesthetic action was unclear, due to the lack of knowledge and instrumentation available to researchers. From 1899 to 1997 there have been four leading hypotheses of anesthetic action: the Meyer – Overton Correlation (1899),⁶ the Critical Volume Model of the Lipid Hypothesis of General Anesthetic Action (1973)¹⁷, the Membrane Protein Hypothesis of General Anesthetic Action (1984)¹⁸, and most currently the Modern Lipid Hypothesis (1997)⁷. The latter two hypotheses are found in the current literature.^{7,19}

The Meyer – Overton hypothesis was developed independently by Hans Horst Meyer in 1899⁴ and by Charles Ernest Overton in 1901⁵. Each scientist found that general anesthetic potency was proportional to the solubility of the anesthetic in a hydrophobic solvent, (olive oil) which was in contact with hydrophilic region (water) causing a water-oil interface.⁴⁻⁶ This oil-water interface mimicked the cell wall – cytoplasm interface in the body. Meyer and Overton determined that this relationship occurred regardless of whether administration was by inhalation or intravenous. The important quantity was the final concentration of the anesthetic in the lipid membrane. Pohorille *et al.* (1998) have concluded that the product of the partition coefficient of a specified anesthetic dissolved in a nonpolar solvent and its specific anesthetizing partial pressure (the partial pressure of anesthetic in the blood stream required to induce clinical anestitization) is constant for all anesthetics.⁶ Hence, different anesthetics will produce anesthesia at different concentration as each other in the lipid bilayer because it is not the concentration that is important but rather the volume that interacts within the membrane.²⁰

Koblin and colleagues (1990) supported the hypothesis when they reported that 26 different conventionally inhaled anesthetics that were previously reported to have potencies differing by as much as six orders of magnitude had the product of the anesthetizing partial pressure and the partition coefficient equal to each other.²¹ Similar results were observed in three different animal models (mice, dogs, and humans) from the same research group.²¹ As studies continued, the theory that anesthetics penetrate the lipid membrane to access the interior of the cell to cause anesthesia by interacting with neurons began to lose its acceptance. These doubts were supported when research had shown that molecules structurally and or chemically similar to the known anesthetic drugs did not cause anesthetic effects. After 60 years of research, the model of anesthetic action is split between two lipid solubility theories. These are the Meyer – Overton hypothesis, where the anesthetic effect is dependent on the molar concentration in a specific cell, and not on the actual anesthetic itself.²² The other hypothesis is that the plasma membrane experiences an increase in fluidity, which is when the hydrophobic regions of the membrane are caused to expand past the critical volume, upon interactions with anesthetics.²²

Miller and colleagues have theorized that anesthesia occurs when the hydrophobic regions of the plasma membrane expand beyond a critical volume due to the absorption of inert anesthetics molecules.²² The critical volume is defined by the fractional volume of anesthetic to weight of recipient that is needed to cause full anestitization with lack of recovery (EC₅₀ values). They refer to their hypothesis as the critical volume model. While the Meyer – Overton theory takes into account the molar concentration, the critical volume theory takes into account the volume fraction solubility in the cell membrane, this means that the researcher is accounting

for the amount of the anesthetic in the plasma membrane not what was administered in to the blood stream.

Anesthetics are a structurally diverse group of organic molecules that include but are not limited to barbiturates, alcohols, halogenated alkanes, ethers, and some steroids. Most anesthetic agents are low boiling point liquids that easily volatilize at atmospheric pressure and are insoluble in aqueous solutions. However, some anesthetics, such as barbiturates, are soluble in aqueous solutions. Researchers have shown that these anesthetics fluidize not only synthetic phosphatidylcholine – cholesterol lipid bilayers but also some biological membranes; especially those of the neuron.²³⁻²⁷ Similar yet larger organic molecules, for instance larger alkanols or halogenated alkanes, do not fluidize lipid bilayers or biological membranes, and they do not exhibit anesthetic behavior.²⁴ Miller and Pang determined that a difference in lipid composition was a factor that aided in the ability of a molecule to cause an anesthetic effect. This would allow for a plausible mechanism to be formulated for the depression of neuronal function in individuals who are in a state of anesthesia.¹⁷ The authors found that lipid bilayers that have 4 – mole % phosphatidic acid, 33 – mole % cholesterol and the remainder 63 – mole % phosphocholine mimic the biological nerve membrane. Synthetic membranes of this composition are affected by anesthetics and fluidize in their presence.^{17,24,25}

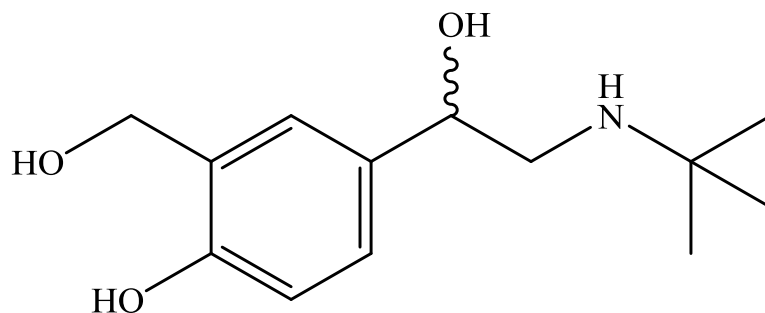
While anesthetics are referred to as non-specific drugs, they must have some pharmacological specificity through attraction of membrane processes, such as the Na^+/K^+ ATPase pump of red blood cells²⁶ or that of the synaptosome.²⁷ These processes, however have been reported to be unaffected by anesthetics, even at levels that should cause lysing of

anesthetic fluidizing cells. The work done by Miller and Pang shows that fluidizing efficacy, which is the rate of change of membrane fluidity in comparison to the concentration of the anesthetic administered, is now needed to fully understand the mechanism of the lipid solubility of anesthetics.¹⁷ Hence, to know the magnitude of fluidizing efficacy or the rate of change of membrane fluidity with concentration of the anesthetic in the membrane needed to enter the lipid membrane to cause enough perturbation in order for anesthetic effects to occur can only be evaluated when the membrane partition coefficient of the particular anesthetic is known.¹⁷

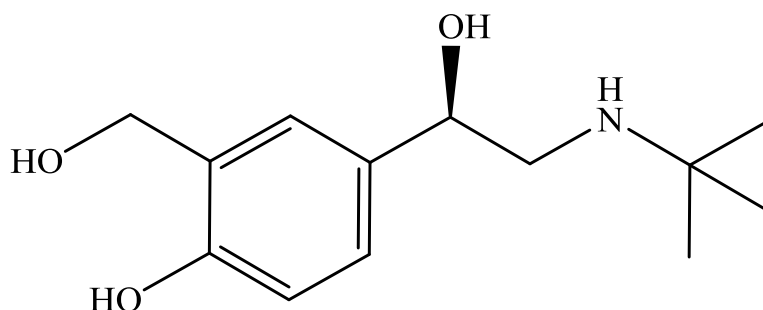
Anesthetics can only act on regions of the membrane that exhibit positive fluidizing efficacies, this can account for the selectivity of the anesthetics for neuronal cell membranes over the membranes of red blood cells. However, when looking at biological cells this straightforward calculation is often complicated by one of two limitations; the first being that there must be transmembrane proteins in the membrane that can alter the fluidization efficacy of the membrane²⁸ or second, that the lipids are distributed heterogeneously across and in the plane of the membrane.²⁹ The fact that membrane spanning proteins can affect the fluidization of the membrane was one of the first indications that membrane protein(s) might play a role in the action of anesthetics.

While these two hypotheses were operating for over 70 years, they had four common weaknesses. One issue is that, stereoisomers while having identical partition coefficients into the lipid membrane, exhibit enantiomer-specific anesthetic effects³⁰. For example albuterol (2-(hydroxymethyl)-4-(1-hydroxy-2-tert-butylamino-ethyl)-phenol) (Figure 1.2 A) contains both enantiomers and Xopenex[®] (4-[2-(tert-butylamino)-1-hydroxyethyl]-2-(hydroxymethyl)phenol)

(Figure 1.2 B) only contains one, hence Xopenex[®] have far less side effects on the cardiovascular and pulmonary system than does albuterol.



(RS)-4-[2-(tert-butylamino)-1-hydroxyethyl]-2-(hydroxymethyl)phenol



4-[(1R)-2-(tert-butylamino)-1-hydroxyethyl]- 2-(hydroxymethyl)phenol

Figure 1.2: A. Albuterol has 2 stereoisomers one of which causes undesirable side effects B. Xopenex[®] contains the purified R isomer of albuterol.

Another issue not addressed by the plasma membrane hypothesis is the ability of chemically similar compounds to produce analgesia and amnesia but not immobility. Some compounds produce convulsive effects indicating that these drugs not only mediate interactions within the central nervous system but also in the peripheral nervous system.³¹ There is also a cutoff effect

that needs to be accounted for. The addition of methylene groups to anesthetic and anesthetic-like molecules can increase the solubility of these compounds in non-polar media, which in essence should increase anesthetic effects. Pringle et *al.* observed that there is a limit to the effectiveness of this strategy.³² The plasma membrane hypotheses focus on changes in membrane fluidity, Franks and Lieb have reported that changes in membrane fluidity due to pharmacologically relevant concentrations of anesthetics are so small that similar changes can be seen by increasing the environmental temperature of membrane by 1° C.³³ Such changes in temperature fall within physiologically observed variations. If anesthetics cause an increase in fluidity equivalent to 1° C, the viability of the critical volume hypothesis is called into question. The mechanism of anesthetic action thus remains open to question and there is credence in the possibility that membrane bound proteins are involved in mediating anesthetic action.

Franks and Lieb have reported that the mechanism of general anesthetic action is governed by competitive interactions with endogenous ligands at the active binding sites for specific receptors.¹⁸ They studied the effects of anesthetics on membrane bound proteins in crystalline structures completely free of lipids and other cellular structures. In that work the authors studied the transmembrane protein Luciferase, which, when combined with luciferin in the presence of adenosine triphosphate (ATP), Mg^{2+} , and O_2 is formed with the emission of a photon.¹⁸ Their data were consistent with a competitive mechanism of action for luciferin and anesthetic at the active site at the protein,¹⁸ Over the next decade research continued to support the mechanism that general anesthetics bound directly to transmembrane ligand – gated ion proteins to cause the anesthetic effect. In a review article, Franks and Lieb concluded that stereospecific general anesthetic isomers had an effect on ligand-gated ion channels such as the glutamate receptor, the

nicotinic acetylcholine receptor, and γ -aminobutyric acid A (GABA_A) receptor families.¹⁹

Support for this mode of action for anesthetics binding to proteins is found in the mechanism of operation for other pharmaceuticals. A host of drugs bind directly to target proteins to produce the desired effect as well as some other undesirable effects.¹⁹

The modern lipid hypothesis proposed by Cantor considers lateral pressure profiles in membranes.⁷ Most likely anesthetics interact with transmembrane proteins causing an inhibition of the ligand – gated ion channel in proteins.⁷ In this model, Cantor discusses that if the ion channel does not open due to the binding of the anesthetic then the area of the membrane where the ion channel should open will increase in cross – sectional area closer to the aqueous interface than in the interior of the membrane causing a change in the lateral pressure of the membrane since their measured change in cross sectional area is greater than the aqueous lipid interface than at the center of the lipids where the acyl chains interact.⁷ This hypothesis is supported by lateral pressure profiles constructed via thermodynamic analysis of synthetic lipid bilayers. While Cantor's research provides a plausible hypothesis, he neglected to add proteins to his bilayers or use real cellular membranes and he still referenced that the anesthetics most likely bind to the proteins; therefore, the leading hypothesis of anesthetic action is that they interact with ligand – gated ion channel proteins.

Ligand – gated ion channels are the simplest membrane – bound protein channels that open or close upon the binding of the specific ligand. These ion channels mediate the flow of ions across the membrane through either a specific or nonspecific ion pore. The flow of ions across a membrane causes secondary messaging systems to operate leading to multiple conscious and unconscious mediations of physical responses from breathing, memory, and heart rate to name a

few. Therefore, the ability to cause known modulations in macroscopic responses like the depression of memory, pain, and movement with anesthetics is advantageous to the medical and research communities for surgeries, but the microscopic cellular level operation of these compounds remains to be understood. It is important to determine if anesthetics cause perturbations in the lipid polar head group region of membranes, if the perturbations occur in the non-polar acyl chains region, or if the interactions between anesthetics and plasma membranes do not involve the bilayer structure directly.

Recent work has suggested anesthetic interactions with proteins in the cell membrane with either animal model or cell lines. Researchers investigating anesthetic interactions with transmembrane proteins are doing so *in vivo*, *in vitro*, and *ex vivo*. The model organism is either the Sprague Dawley or Wistar rat, with the cortex or hippocampus regions used for experiments. These regions were chosen because they are rich in the ligand – gate GABA_A receptors. Hirota *et al.* reported that, using square waveform electrophysiology measurements on harvested rat hippocampus that were transversely sliced at thicknesses 400 nm, an enhanced release of the ready reserve pools of GABA vesicles from the presynaptic terminal was seen upon treatment with intravenous (IV) anesthetics.³⁴ The anesthetics used were sevoflurane (Figure 1.3 A), isoflurane (Figure 1.3 B), thiopental (Figure 1.3 C), pentobarbital (Figure 1.3 D), and nipecotic (Figure 1.3 E); the first two are inhalation anesthetics and the latter 3 are IV anesthetics.³⁴

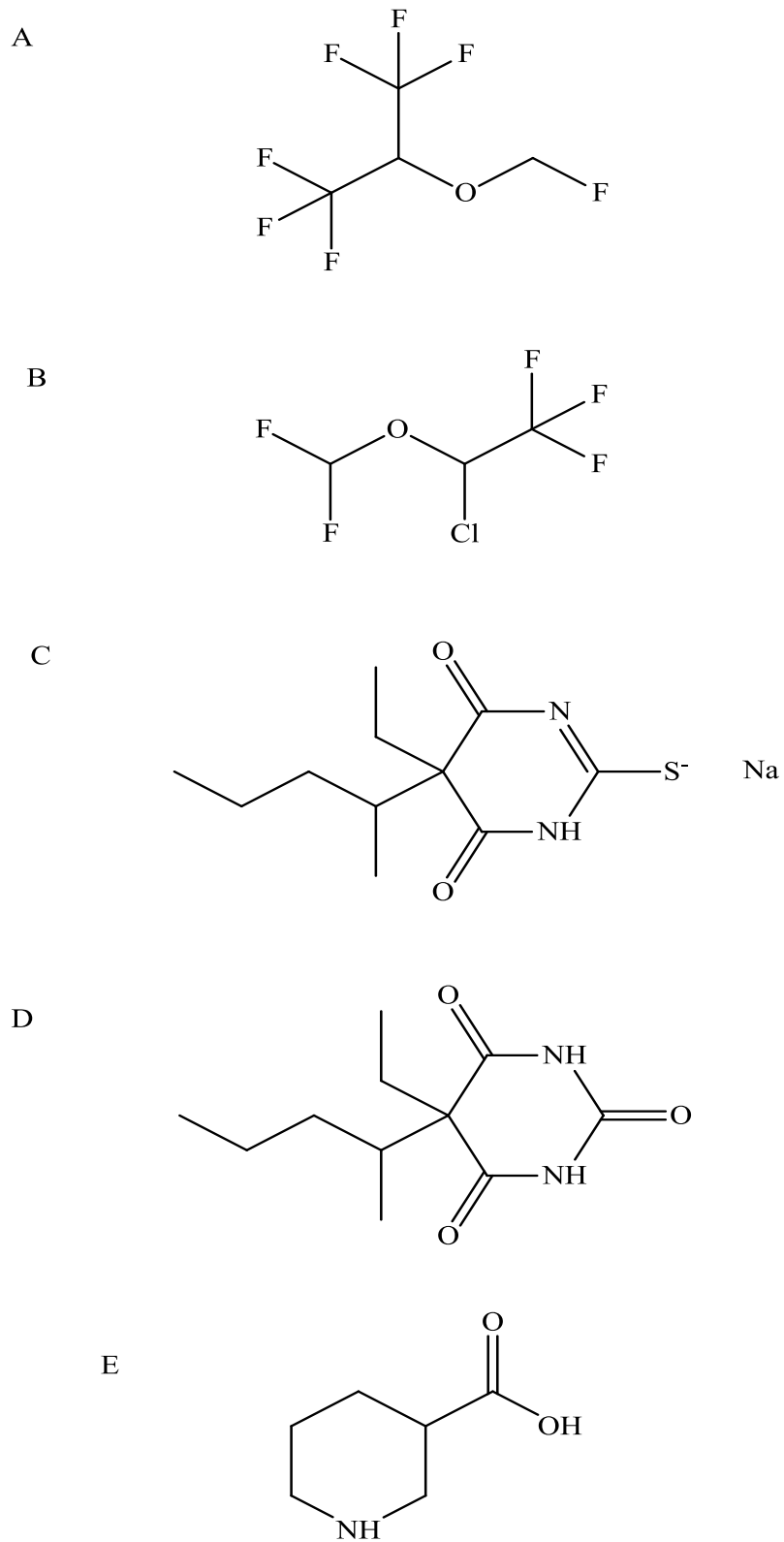
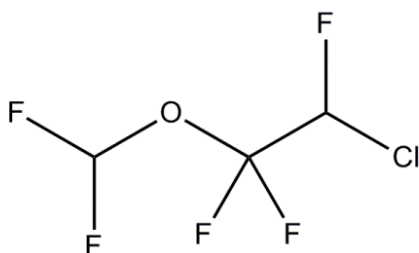


Figure 1.3: A. Sevoflurane; B. Isoflurane; C. Thiopental; D. Pentobarbital; E. Nipecotic.

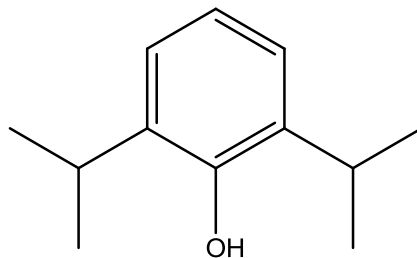
These findings may explain why individuals who are anesthetized frequently due to multiple surgeries from trauma are more often unsuccessfully immobilized. GABA is the principal inhibitor in the CNS and, when there is a larger release of GABA in the synaptic cleft due to the action of anesthetics, the clearing or decay time of GABA from the cleft is slowed, allowing a greater response to GABA. The Akaike group investigated the effects of volatile anesthetics on isolated GABA synapsis from Wistar rats using whole cell patch clamp electrophysiological techniques.³⁵ They harvested the hippocampus of rats, which was kept in ice cold oxygenated (O₂) artificial cerebral-spinal fluid (aCSF) until 400 nm thick sections were taken for patch clamp measurements.³⁵ Sevoflurane (Figure 1.3 A), isoflurane (Figure 1.3 B), and enflurane (Figure 1.4) all enhanced the exogenous levels of GABA upon stimulation.³⁵



(RS)-2-chloro-1-(difluoromethoxy)-1,1,2-trifluoro-ethane

Figure 1.4: Structure of Enflurane.

Anesthetics cause an increase in chlorine ions to pass into the neuron through the GABA_A receptor which causes the GABA_A receptor to become inhibited, but the mechanism by which this occurs is unknown. Turina posed a plausible explanation with the use of the drug propofol. Propofol (2, 6-diisopropylphenol) (Figure 1.5) causes a narrowing of the neuritis by causing an increase in the contractibility of myosin of the GABA_A receptor.



2,6-diisopropylphenol

Figure 1.5: Propofol is a commonly used barbiturate anesthetic for both animals and humans.

This narrowing causes a measurable response of the GABA-filled vesicles that were reported to have a change in direction and increase in velocity of neurotransmitter release from the docked vesicle towards the cell body instead of into the synaptic cleft. These data were collected using cortex tissue harvested from newborn Sprague Dawley rats. The harvested tissue was kept alive with warmed O_2 – artificial cerebral spinal fluid (aCSF) while being monitored with video microscopy.³⁶ The narrowing of the neuritis via the increase in the contractibility of myosin of the $GABA_A$ receptor was observed only on the harvested cortex tissue but when the $GABA_A$ receptor antagonist gabazine showed a reversal of the effects of the propofol. The authors state that their work is a step in the direction of understanding the mechanism of anesthetic action but further investigation is needed.³⁶ These are initial steps in determining the mechanism of anesthetic action. A broad selection of anesthetics will need to be investigated before commonality in two models of action can be resolved. This is further supported by the fact that GABA receptor itself has four subunits of interaction are the α_1 , α_2 , γ and β_1 subunits. The ribbon structure of the $GABA_A$ receptor is shown in Figure 1.6.

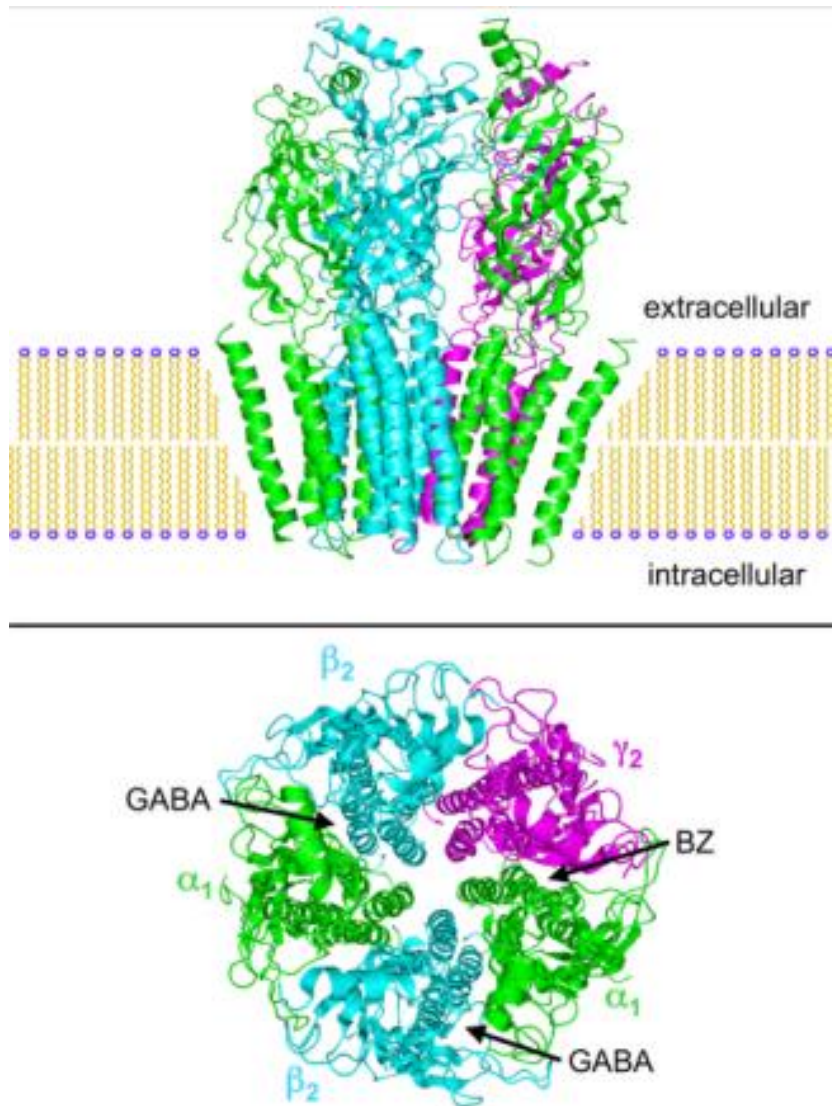
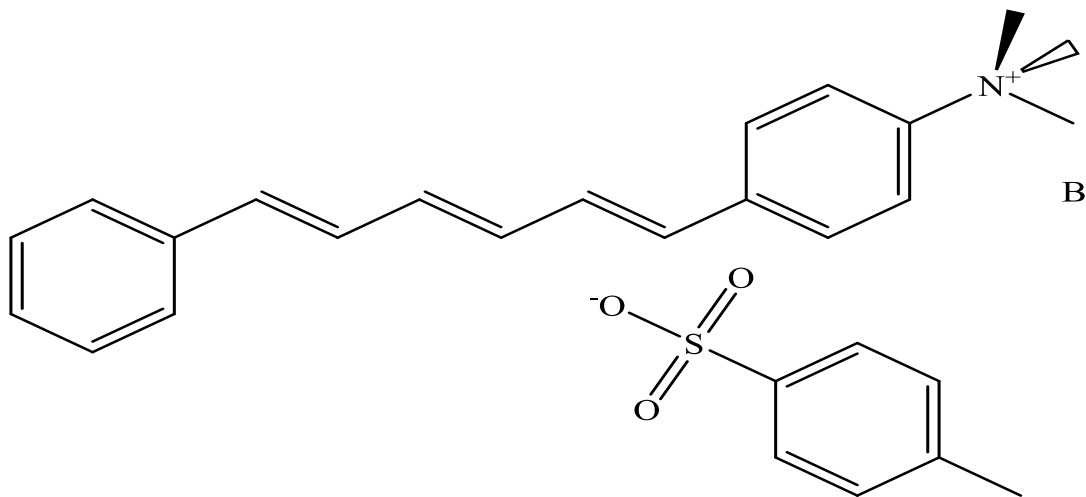
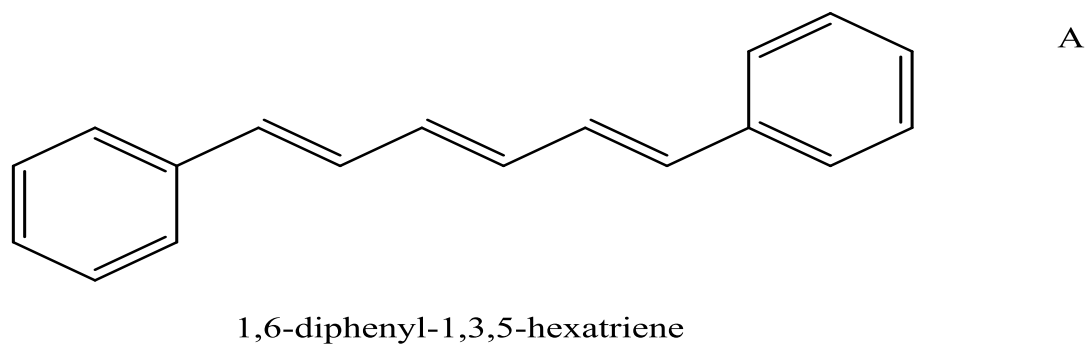


Figure 1.6: Refined structure of the GABA_A receptor at 4Å resolution. Unwin, N., (2005)

J.Mol.Biol.346: 967. For interpretation of the references in color in this and all figures, the reader is referred to the electronic version of this thesis.

Despite this evidence, the role of anesthetic interactions directly with lipid bilayers cannot be ruled out. Nelson et al. (2012) investigated lateral pressure changes in the head and tail regions of DPPC liposomes when dosed with isoflurane with two fluorescent chromophore using

steady state fluorescence anisotropy measurements.³⁷ Anisotropy decay measurements is an experimental result that gives rise to how fast a chromophore orientates and diffuses out the local environment in the Cartesian component axis of X, Y, and Z. Vesicles were formed using extrusion with 1,6-diphenyl-1,3,5-hexatriene (DPH) (Figure 1.7 A) or N,N,N-Trimethyl-4-(6-phenyl-1,3,5-hexatrien-1-yl) phenylammonium *p*-toluenesulfonate (TMA – DPH) (Figure 1.7 B) as probes and 1,2-dihexadecanoyl-*sn*-glycero-3-phosphocholine (DPPC) as the phospholipid (Figure 1.8) in an isoflurane solution prepared in 4-(2-hydroxyethyl)-1-piperazineethanesulfonic acid (HEPES) buffer.



N,N,N-trimethylamino-4-(6-phenyl-1,3,5-hexatrien-1-yl) phenylammonium *p*-toluenesulfonate

Figure 1.7: A. DPH is a non-polar chromophore; B. TMA-DPH is polar

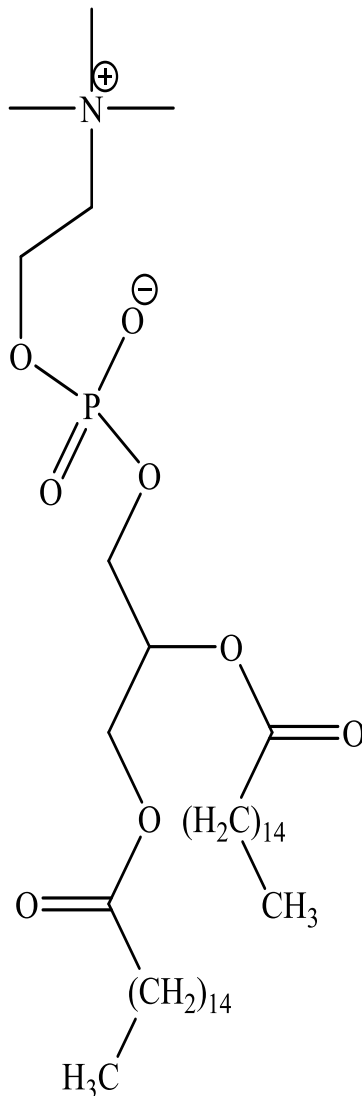


Figure 1.8: Structure of DPPC

The Nelson group reported an increase of 0.2 in the steady state fluorescence anisotropy value for TMA – DPH vesicles and a similar decrease in the steady state fluorescence anisotropy value of DPH-containing vesicles when the vesicles were treated in 7 – 25 mM isoflurane baths.

³⁷ The authors attribute the increase in non - axial dye mobility in the tail region and the decrease in the head region to the lateral pressure changes in the membrane associated with the interaction of the anesthetic. ³⁷ While this information has provided some insight into the

mechanism of general anesthetic action, much remains to be done. A key step in understanding anesthetic action is to resolve whether or not the primary chemical interactions are between anesthetic and the lipid bilayer or between anesthetic and transmembrane proteins. We are poised to evaluate whether or not anesthetics interact with lipid bilayers using time resolved fluorescence lifetime and anisotropy decay measurements. These measurements provide significantly more molecular-scale insight into probe-lipid interactions than can be obtained with steady state fluorescence anisotropy measurements.

The goal of this research is to investigate the interaction of general anesthetics with synthetic lipid membrane and to identify changes in the organization of the lipid membrane. The Modern Lipid Hypothesis was investigated with the use of synthetic vesicles. The Membrane Protein Hypothesis of General Anesthetics was not investigated here due to experimental complexity. Lipid bilayers in the form of vesicles were made to mimic the neuronal cell plasma membrane. The vesicles were unilamellar of a controlled size of 400 nm. These vesicles were constructed with one of two probes so that either the polar head regions of the lipids or the non-polar acyl tail regions were interrogated by rotational diffusion of the probes.

Synthetic vesicles are produced by extrusion, as described previously.³⁸ The composition of 63 – mole % phosphatidylcholine (PC), 4 – mole % phosphatidic acid (PA) with 33 – mole % cholesterol is used in the synthetic vesicles studied in this work. The PC that will be used to make the synthetic vesicles is 1, 2-dihexadecanoyl-*sn*-glycero-3-phosphocholine (DPPC) (Figure 1.8). Two different chromophores will be used to investigate anesthetic identity- and concentration-dependent changes in the vesicle head group and acyl chain regions. These are (N-(7-nitro-2,1,3-benzoxadiazol-4-yl) (NBD),) 1,2-dioleoyl-*sn*-glycerol-3-phosphoethanolamine N-(7-nitro-2,1,3-benzoxadiazol-4-yl) (ammonium salt) (Figure 1.9),

and perlyene (Figure 1.10). The phosphatidic acid (PA) used is 1,2-dihexadecanoyl-*sn*-glycerol-3-phosphate (sodium salt) (DPPA) (Figure 1.9). Cholesterol (Figure 1.11) was obtained from ovine wool. These vesicle constituents were chosen to model qualitatively the composition of neuronal cell plasma membranes based on the work of Botchway *et al.*³⁹

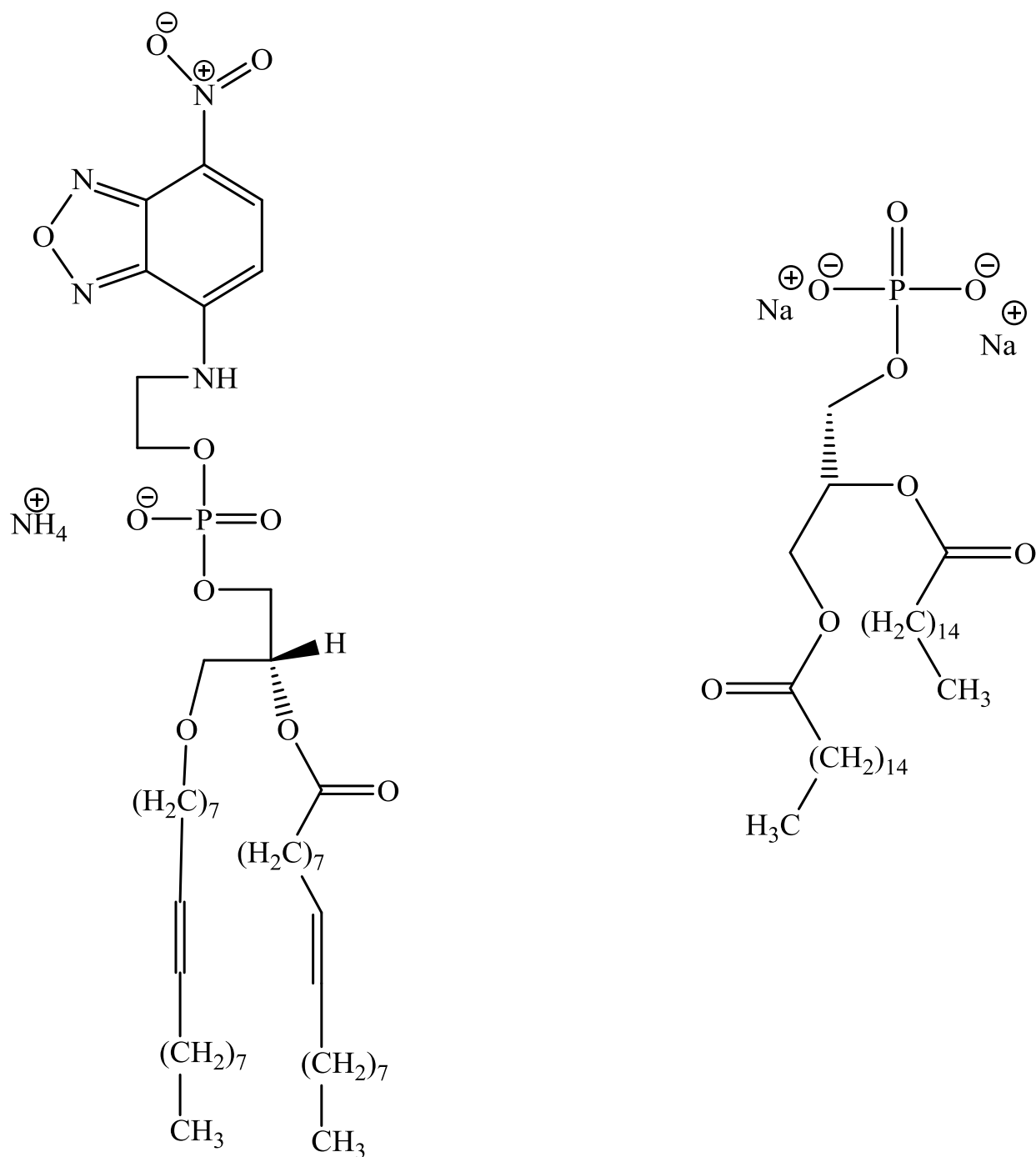
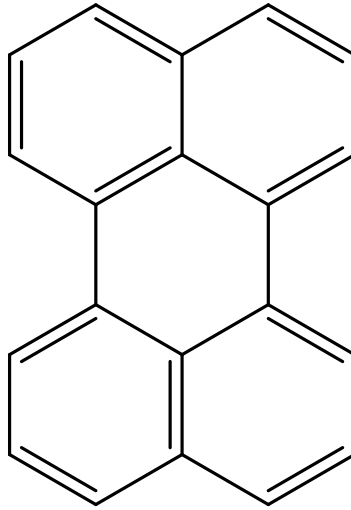


Figure 1.9: Left DPPE with an NBD chromophore tag, 1,2-dioleoyl-*sn*-glycero-3-phosphoethanolamine-N-(7-nitro-2-1,3-benzoxadiazol-4-yl) (ammonium salt). Right DPPA, 1,2-dihexadecanoyl-*sn*-glycero-3-phosphate (sodium salt).



perylene

Figure 1.10: Structure of Perylene.

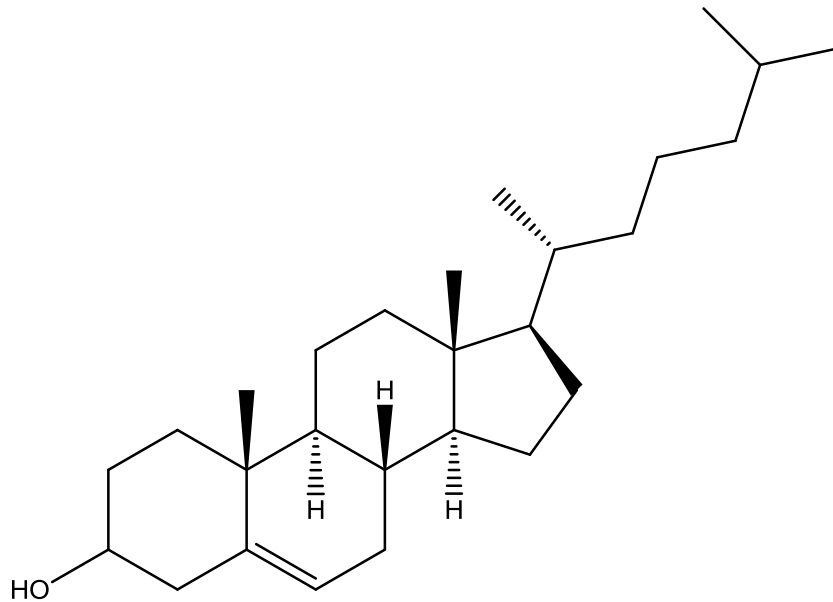


Figure 1.11: Structure of Cholesterol.

Fluorescence is a radiative emission process that occurs as a result of the excitation of a sample by absorption of a photon. Optical absorption is described using Beer's Law,

$$A = \epsilon bc \tag{1.1}$$

where A is the absorbance, ϵ is the molar absorptivity (L (mol cm)^{-1}), b is the path length of the cell (cm) and c is the concentration of the absorbing species (mol L^{-1}). Upon excitation, radiative emission can occur as either fluorescence (short lifetime; $< 10^{-5}$ s) or as phosphorescence (long lifetime; seconds to minutes). The difference between these two emission processes is that with fluorescence the electronic energy transitions do not involve a change in electron spin, hence the shorter lifetime. This emission of radiation as a photon occurs at wavelength longer than that of the excitation photon.

Factors that can affect fluorescence intensity are transition type, chromophore structure and rigidity, system temperature, pH, concentration, and dynamic quenching.⁴⁰ Fluorescence quantum efficiency is the ratio of the radiative rate constant to the sum of all rate constants for relaxation from the excited state. The rate constants that can contribute include the radiative rate constant, (k_r), intersystem crossing (k_{in}), external conversion (k_{ec}), internal conversion (k_{ic}), predissociation (k_{pd}), and dissociation (k_d).⁴⁰ The individual rate constants are related to fluorescence quantum yield according to equation 1.2.

$$\phi = \frac{k_r}{k_r + k_{in} + k_{ec} + k_{ic} + k_{pd} + k_d} \quad (1.2)$$

The magnitude of each rate constant depends on the chemical structure of the chromophore and the environment. Molecules that have aromatic functional groups, aliphatic and alicyclic carbonyl structures or those molecules that have highly conjugated double bonding character are typically characterized by a dominant $\pi \rightarrow \pi^*$ transition and in many instances they are observed

to emit.⁴⁰ Factors that can reduce fluorescence quantum yield include the presence of halogen substituents on ring structures. In relation to structure, planar, rigid chromophores often exhibit a high fluorescence quantum yield because of the optimization conjugation and minimization of access to nonradiative decay channels.⁴⁰ For such chromophores, fluorescence intensity is typically temperature dependent. Increased temperature provides increased system energy that will reduce the viscosity of the solution and increase the frequency of collisional interactions that can result in energy transfer or internal conversion. Compounds that have acidic or basic ring substituents can exhibit pH-dependent fluorescence intensity because protonation/deprotonation will alter the nature of π -conjugation in such systems.

As indicated above, for a molecule to fluoresce it must first absorb a photon and since absorption is related to concentration then fluorescence is also dependent on concentration. Beer's law can also be expressed as⁴⁰

$$\frac{P}{P_0} = 10^{-\epsilon bc} \quad (1.3)$$

where P is the power of the exciting light beam after passing through the cell of path length b , and P_0 is the incident power of the exciting light beam. Fluorescence can be related to equation 1.3 through⁴⁰

$$F = K' P_0 (1 - 10^{-\epsilon bc}) \quad (1.4)$$

where F is the fluorescence intensity, K' is a proportionality constant to account for geometric and electronic details of the particular instrument being used, K' in fact, is instrument dependent

and the quantum efficiency, and ϵbc is the absorbance. Equation 1.4 is valid over a limited concentration range. Deviations from the relationship between fluorescence intensity and chromophore concentration can arise due to collisional quenching or aggregate formation, for example. These factors need to be taken into account when choosing probes and probe concentrations for fluorescence spectroscopy measurements.

NBD has a fluorescence lifetime that is sensitive to the dielectric properties of the local environment this means that in a polar environment it will have a shorter fluorescence lifetime than in a non-polar environment. The anesthetics in question are characterized by a dielectric response that is different than either an aqueous environment or a nonpolar environment. When anesthetics interact with lipids or cholesterol, the dielectric response of the modified environment will be changed and if this change occurs in close proximity to the NBD chromophore, a change in fluorescence lifetime and also possibly reorientation time will be seen. Any change in chromophore reorientation time was observed for a nitroxide reporter group tethered to the PC by Miller and Pang for range of anesthetics that include but are not inclusive to pentobarbital and halothane in synthetic lipid membranes. The NBD chromophore is excited at 450 nm and has an emission maximum at 530 nm.¹⁷ For the interrogation of the non-polar acyl chain region of our vesicles, we use perylene as a probe molecule. Studies from Lapinski and Blanchard showed that in vesicles ranging from 100 – 1000 nm the chromophore perylene orientated itself in the acyl chain regions of unilamellar vesicles.⁴¹ Perylene was chosen because it is a non-polar, rigid polycyclic hydrocarbon that does not exhibit anomalous spectroscopic behavior such as strong vibronic coupling or intensity borrowing,⁴² and has a fluorescence lifetime that is well matched to the rotational diffusion times measured in this work.

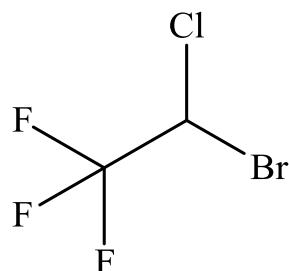
Perylene is excited at 444 nm exhibits prominent emission in the vicinity of 470 nm. When the saturated PC and PA lipids are in an ordered phase and perylene is located within this region, relatively slow rotational diffusion motion is measured. Interactions between anesthetics and the acyl chain region of the lipid bilayer will serve to decrease the organization of the acyl chains, providing more rotational freedom for perylene, resulting in faster reorientation times.

To gain some measure of insight into the effects of anesthetics on the lipid membrane, three anesthetics have been chosen for examination: barbiturates, ethers and halogenated alkanes. The specific anesthetics are pentobarbital (5-Ethyl-5-(1-methylbutyl)-2,4,6(1*H*,3*H*,5*H*)-pyrimidinetrione) (Figure 1.3 D),^{43,44} isoflurane (1-chloro-2,2,2-trifluoroethyl difluoromethyl ether) (Figure 1.3 B) and halothane (1-bromo-1-chloro-2,2,2-trifluoro-ethane) (Fig. 1.10).⁴⁴

Information on the properties of these anesthetics, including molecular weight, boiling point, and the Oswald solubility coefficients can be found in Table 1. While the modes of activity of the anesthetics are thought to be different, there remains much detail to be determined as to the molecular interactions that characterize the anesthetic-lipid system. The impact of this work will show whether anesthetics interact with the plasma membrane without transmembrane protein and if they do where interactions are greatest: in the polar or non-polar regions on the bilayer. Also, this work will be a stepping stone to help bridge the Modern Lipid Hypothesis with that of the Membrane lipid Hypothesis of General Anesthetics.

As one can conclude there are significant risks when undergoing anesthesia. Even the most skilled and trained anesthesiologist may have problems with a patient that is considered healthy since the mode(s) of action of these drugs remains to be understood in detail. Their effects are not only on the CNS but also in the peripheral nervous system, with effects on the heart, lungs, and gastrointestinal tract. It is important to elucidate the interactions between

anesthetics and model lipid bilayers to advance our knowledge of the mode(s) of operation of anesthetics.



1-bromo-1-chloro-2,2,2-trifluoro-ethane

Figure 1.12: Structure of Halothane.

Name of Inhaled Anesthetic	MW (Da)	BP (degree C) at 1 atm	SVP at 20 C (kPa)	MAC (% v/v)	Ostwald Solubility Coefficients					
					O/W	Bl/G	W/G	Br/G	O/G	Br/Bl
Halothane	197	50.2	32.5	0.75	220	2.3	0.8	4.8	224	1.9
Isoflurane	184.5	48.5	31.9	1.15	174	1.43	0.62	21	91	1.6

Table 1.1: Summary of properties of the inhaled anesthetics halothane and isoflurane. MW - molecular weight, BP - boiling point, SVP - saturated vapor pressure, MAC - minimal alveolar concentration, O/W - oil water, Bl/G - blood gas, W/G - water gas, Br/G - brain gas, O/G - oil gas, Br/Bl brain blood interfaces⁴⁴

CHAPTER 2

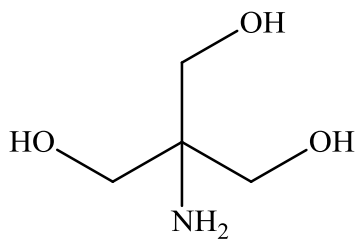
EXPERIMENTAL PROCEDURES

Current investigations on the mechanism of anesthetic interactions with the central nervous system (CNS) have taken two approaches. One group of investigations utilizes cell lines and/or animal models, and another body of work uses synthetically prepared vesicles. Groups who use cell lines and/or animal models do so, on the premise that anesthetics interact with the ligand – gated ion channels (LGIC) imbedded in the lipid membrane. Upon interaction of the anesthetic with the LGIC, there are changes in the membrane and with neurotransmitter (NT) release. There is also another school of thought, based on the range of chemical structures that give rise to outwardly similar anesthetic effects. For this reason, the processes of primary concern are the interactions between the lipid membrane and the anesthetics, with such interactions giving rise to changes in lipid membrane order or permeability, which lead to changes in NT release. A connection can be made between these two possibilities. We use synthetically prepared vesicles that mimic the neuronal lipid membrane composition without having the complexity of LGIC structures in them. With the use of these model bilayer systems we can investigate the fluidity and extent of organization of the bilayer as a function of exposure to different anesthetics. We measure the fluorescence lifetime and induced orientation anisotropy decay of a chromophore in the membrane using time – correlated single – photon counting (TCSPC). These experiments are designed to determine the details of interactions between anesthetics and the lipid bilayer membrane. If anesthetics interact directly with the lipid membrane, there will be changes in the organization and local inter-molecular frictional interactions, and these changes will be reflected in the rotational diffusion dynamics of the probe

residing in the lipid bilayer acyl chain region. We provide detailed information in this Chapter on the experimental details of these measurements.

Vesicle Preparation: Vesicles were formed by extrusion from mixtures containing phospholipid, sterol and chromophore species in predetermined amounts. The formation of vesicles from mixtures of these components is driven entropically to produce structures where interactions between polar solution and nonpolar organic constituents are minimized. The vesicle constituents 1,2-dihexadecanoyl-*sn*-glycero-3-phosphocholine (DPPC), 1,2-dioleoyl-*sn*-glycerol-3-phosphoethanolamine N-(7-nitro-2,1,3-benzoxadiazol-4-yl) (ammonium salt) (18:1 NBD-PC), 1,2-dihexadecanoyl-*sn*-glycerol-3-phosphate (sodium salt) (DPPA), and cholesterol were purchased from Avanti Polar Lipids Inc. (Alabaster, AL) in powdered form and were used without further purification. Perylene was purchased from Sigma-Aldrich (St. Louis, MO) and used as received. These constituents were dissolved in 10 mM 2-Amino-2-hydroxymethyl-propane-1,3-diol (TRIS[®]-HCl) – buffer containing 100 mM sodium chloride (Figure 2.1) at pH 7.4, they were then stored at -20°C until use. Both NBD and perylene chromophore-containing vesicle solutions were prepared in 0.3 mM concentrations where 63 mole-% was DPPC, 33 mole-% cholesterol and 4 mole-% DPPA. Vesicles containing 18:1 NBD-PC chromophore had a chromophore concentration of 1 mole-% and vesicles containing perylene had a chromophore concentration of 0.5 mole-%. The TRIS[®]-HCl buffer was prepared using Milli-Q Plus water purification system (Millipore, Bedford, MA). To ensure adequate mixing, the lipid mixtures underwent five freeze-thaw-vortex cycles. Each cycle was a 5 minute immersion in liquid nitrogen, followed by a 5 minute immersion in a 60°C water bath, and a 2 minute vortex. To prepare 400 nm diameter vesicles, these mixtures were extruded eleven times through a polycarbonate membrane with a 400 nm pore diameter (Avanti Polar Lipids Inc.,

Alabaster, AL) in 1 mL increments. It is known from prior work in the Blanchard group that this method of vesicle preparation produces vesicles with the same diameter as the nominal pore size of the membrane.⁴¹ All extrusions were performed at room temperature. A 20 mL aliquot of lipid mixture was used to prepare vesicles by extrusion weekly, and these vesicles were stored at room temperature until used within the same week.



2-Amino-2-hydroxymethyl-propane-1,3-diol

Figure 2.1: Structure of Tris - HCl ®.

Anesthetic Solution Preparation: Pentobarbital, (5-Ethyl-5-(1-methylbutyl)-2,4,6(1*H*,3*H*,5*H*)-pyrimidinetrione), (Figure 1.3 D) was donated by Professor Spence and was purchased originally from Sigma-Aldrich (St. Louis, MO). Isoflurane, (1-chloro-2,2,2-trifluoroethyl difluoromethyl ether), (Figure 1.3 B) was purchased from Phoenix Pharmaceutical Inc. (St. Joseph, MO), and halothane, (1-bromo-1-chloro-2,2,2-trifluoro-ethane), (Figure 1.12) was purchased from Sigma-Aldrich (St. Louis, MO). All anesthetic solutions were prepared weekly in 10 mM or 100 mM stock solutions in Milli-Q water (Millipore, Bedford, MA). These solutions were stored in tightly sealed amber bottles in a dark room.

Steady-State Fluorescence Measurements: Excitation and emission spectra were collected using a Hitachi F-4500 fluorescence spectrophotometer to determine the NBD (Figure 1.7) and perylene (Figure 1.8) absorption and emission band positions in our vesicle

preparations. A spectral band pass of 1 nm was used for both the excitation and emission monochromators for all measurements.

Time-Correlated Single Photon Counting (TCSPC): A time-correlated, single-photon counting instrument was used to acquire time-resolved fluorescence lifetime and fluorescence anisotropy decay data. The details of this system have been described previously,⁴⁵⁻⁴⁷ and only the essential properties will be recapped here. The light source is a CW passively mode-locked, diode-pumped Nd:YVO₄ laser (Spectra Physics Vanguard) that produces ~12 ps pulses at 1064 nm at a repetition rate of 80 MHz. The fundamental wavelength is frequency doubled to produce 2.5 W average power at 532 nm with the same pulse characteristics as the fundamental output. Pulses at 355 nm were generated by mixing the fundamental and second harmonic pulses, producing 2.5 W average power with the same pulse characteristics as with the fundamental and second harmonic output. The second and third harmonic outputs from the Nd:YVO₄ laser excite cavity dumped dye lasers (Coherent 702-2) that operate between 430 – 850 nm. The cavity dumped dye laser produces a 5 ps pulse at a repetition rate of 4 MHz. Average output power of the dye laser is wavelength dependent and is typically in the range of 50 mW to 250 mW. Excitation of the NBD S₁ ← S₀ transition was at 450 nm (Stilbene 420 dye, Exciton), and emission was collected at 530 nm. For perylene, excitation of the S₁ ← S₀ transition was at 440 nm (Stilbene 420 dye, Exciton), and emission was collected at 475 nm. The laser output was linearly polarized with a polarization extinction ratio of *ca.* 100:1. Each polarized excitation pulse is divided into two pulses, with one pulse directed to a reference photodiode (Becker & Hickl PHD-400-N) and the other pulse directed into the sample. Emission from the sample is collected at right angles to the excitation axis using a 40 X reflecting microscope objective (Ealing) and directed to two detection channels. The emission signal is separated into two

polarization components using a polarizing cube beam splitter, parallel (0°) and perpendicular (90°) with respect to the vertically polarized excitation pulse. The separate polarized signal components are detected simultaneously using microchannel plate photomultiplier tubes (MCP-PMT, Hamamatsu R3809U-50). Each photomultiplier tube is equipped with a subtractive double monochromator (Spectral Products CM-112). The parallel and perpendicular transients are recorded separately by two – channel TCSPC detection electronics (Becker & Hickl SPC-132) yielding *ca.* 30 ps response functions for each detection channel. All instrumentation was operated using a LabVIEW[®] (National Instruments) program written in-house. All samples were mixed by inverting 4 times between data acquisitions to minimize photo-bleaching effects. A schematic of the TCSPC instrument is shown in Figure 2.2.

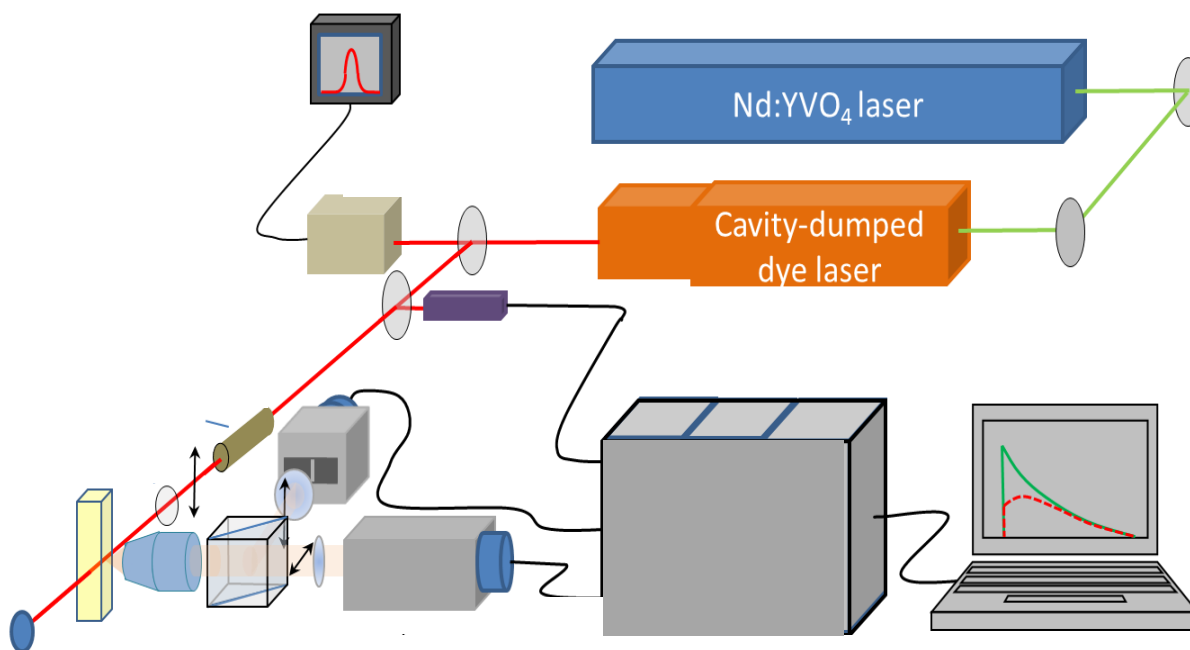


Figure 2.2: Schematic of TCSPC instrument used in this work.

Fluorescence Lifetime and Anisotropy decay: Fluorescence lifetime (τ_{fl}) is the time constant associated with the first-order population decay from the first excited singlet state of a molecule. The rate constant for the relaxation process is given by k:

$$k = k_r + k_{nr} \quad (2.1)$$

where k_r is the rate constant of the radiative decay and k_{nr} is the rate constant of the non-radiative decay. Because the intensity of fluorescence is related directly to the population of the excited state, the time-dependence of the intensity decay is modeled as a first order process. The time constant of the decay is inversely related to the rate constant:

$$\tau(fl) = 1/k \quad (2.2)$$

The time-dependence of first order relaxation is given by equation (2.3)

$$I(t) = I(0)\exp(-t/\tau(fl)) \quad (2.3)$$

where t is time, I_0 is the initial intensity at time zero, and τ_{fl} is the fluorescence lifetime. The fluorescence lifetime is determined by fitting the experimental time domain fluorescence intensity decay to equation 2.3. The excited and emitting transitions can be described with respect to the Cartesian axis system for the chromophore. Molecules absorb light most effectively when the polarization of the exciting electric field is parallel to the orientation of the absorbing transition dipole moment, with the relative efficiency of this process scaling according to Equation 2.4,

$$I(\theta) = 0.5(3\cos^2\theta - 1) \quad (2.4)$$

where θ is the angle between the absorbing transition moment and the polarization of the incident electric field.

In the true domain there are two contributions to the intensity decay of polarized transients. These are the population of excited molecules and their orientation distribution. To separate the contributions of these two processes, the emission intensity decay can be measured at a polarization angle where orientation relaxation does not contribute. For linear processes the angular dependence of emission polarization is given by Equation 2.4, and the magic angle is given by the condition $I(\theta) = 0$. For this condition $\theta=54.7^\circ$.

To extract information from polarized emission transitions on the molecular motion of the excited ensemble, the induced orientation anisotropy function is used

$$R = \frac{I_{\parallel}(t) - I_{\perp}(t)}{I_{\parallel}(t) + 2I_{\perp}(t)} \quad (2.5)$$

The anisotropy decay function is the time resolved difference between polarized emission transients, normalized for total fluorescence intensity as a function of time. Physically this quantity represents the time scale and means by which a non-random distribution re-randomizes. The functional form of $R(t)$ has been treated theoretically and can contain up to five exponential decay components. Experimentally, one or two component decay can be resolved, with the time constants and relative amplitudes of the components provide information on the physical properties of local environment of the chromophore and the shape of the volume it sweeps out. The key to interpreting $R(t)$ data lies in extracting the Cartesian components of the rotational diffusion constant from the exponential decays. This issue is discussed in detail for perylene in Chapter 3.

The simplest model for rotational diffusion was developed in 1929 by Debye, and subsequently modified by Perrin to account for rotor shape, and Hu and Zwanzig to account for frictional interactions between the rotor and its environment. This model indicates that the time constant of the induced orientation anisotropy decay depends on the viscosity of the medium (η),

the shape of the rotating entity (S) (for perylene $S = 0.7$), and the hydrodynamic volume of the rotor (V) ($V = 225 \text{ \AA}^3$ for perylene).

$$\tau_{or} = \frac{1}{6D_{rot}} = \frac{\eta Vf}{k_B T S} \quad (2.6)$$

where τ_{or} is the anisotropy decay time constant, D_{rot} is the rotational diffusion constant, f is a term to account for frictional component of the interactions between the rotor and its environment, k_B is the Boltzmann constant and T is the system temperature.

The time-evolution of the experimental $R(t)$ signal is schematized in Figure 2.2 and in some instances the modified DSE equation (Eq. 2.6) can be applied directly. For other systems, including perylene reorienting in vesicle structures, extracting information on the details of molecular rotational motion is somewhat more involved than the simple application of Eq. 2.6 and we discuss that issue in Chapter 3.

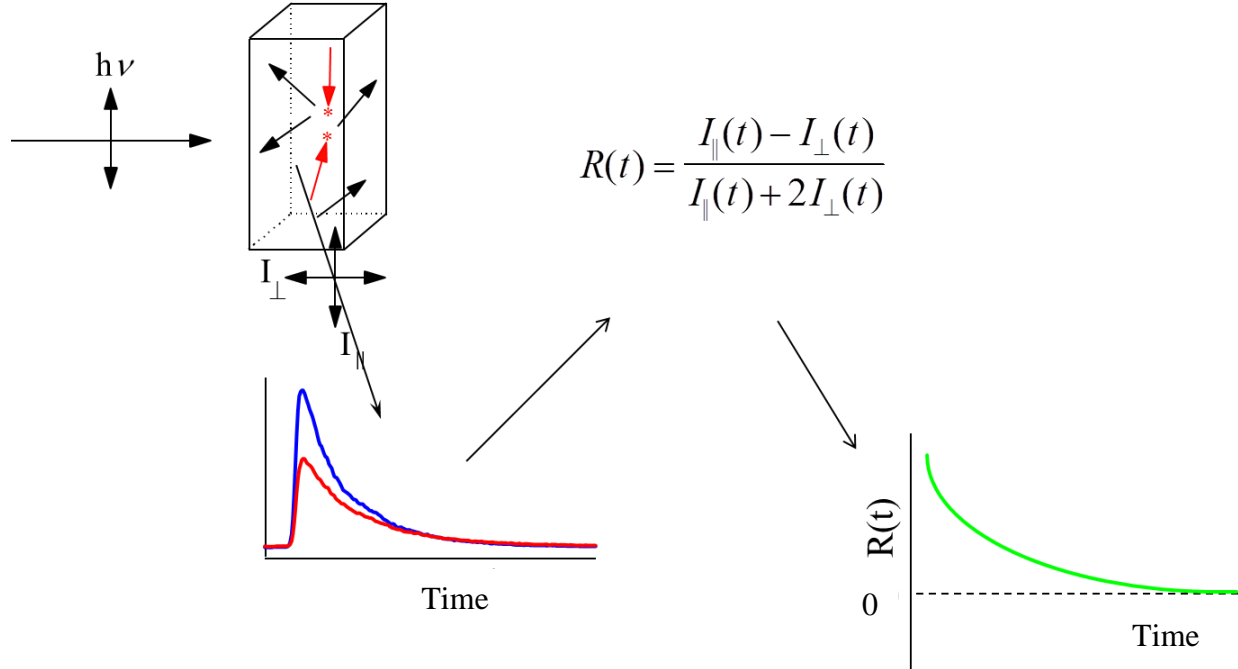


Figure 2.3: Schematic of the principles behind the anisotropy decay measurement.

CHAPTER 3

The central purpose of this work is to understand the manner in which general anesthetics interact with model lipid bilayer structures. There have been a number of mechanisms proposed for the operation of general anesthetics, among them being the hypothesis that general anesthetic molecules interact with lipid bilayer structures in such a way as to disrupt the organization of the bilayer and thus alter the ability of the bilayer to mediate transport processes. It is not clear whether this transport mediation acts through the structure of transmembrane proteins or directly on the bilayer, but the common underlying premise is that the anesthetic molecules interact with the lipid bilayer.

There are a number of means available to characterize the organization of lipid bilayer structures. Among them is the use of fluorescent chromophores imbedded in the bilayer or attached to a bilayer constituent. While fluorescent chromophores can produce local structural perturbations due to their size and/or polarity, their use is well established and much has been learned from their use regarding lipid bilayer structure and dynamics. In this work we have used two fluorescent probes, one attached to the head group of a phospholipid and the other free to partition into the nonpolar region of the bilayer. We have used a phosphoethanolamine-N-(7-nitro-2-1,3-benzoxadiazol-4-yl) (ammonium salt), (NBD) and perylene (Fig. 3.1). The tethered NBD species locates the chromophore in the lipid bilayer polar head group region and perylene, which is not attached to a lipid bilayer constituent, exhibits essentially no solubility in water and partitions exclusively into the bilayer acyl chain region. Acquisition of time-resolved

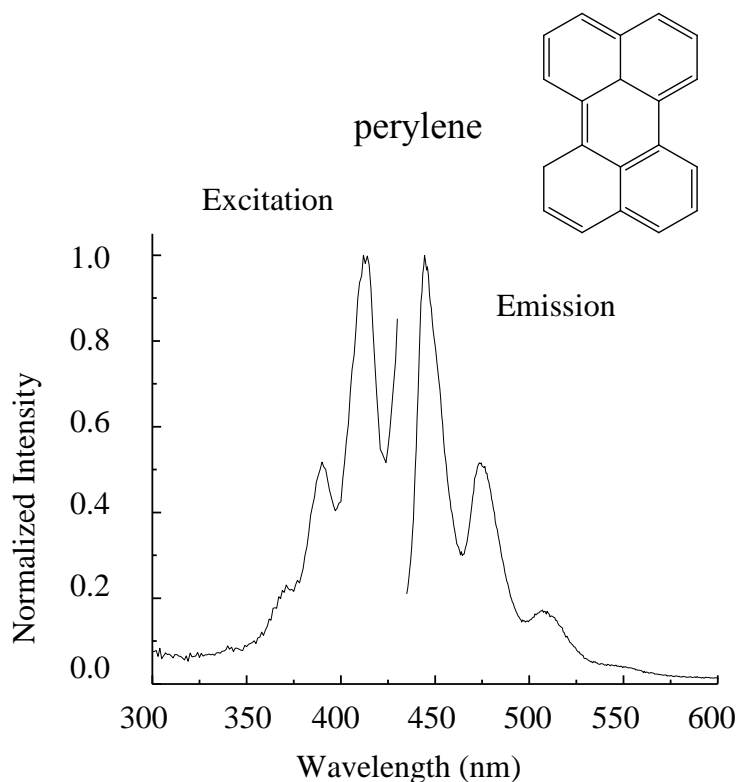


Figure 3.1. Left: Structure, excitation and emission spectra of perylene

fluorescence data from the tethered NBD chromophore as a function of the amount of anesthetic present has shown that this chromophore is not sensitive to the presence of anesthetics. This is not a surprising result owing to the polarity of the region in which the NBD chromophore resides. Perylene, which incorporates exclusively into the lipid bilayer acyl chain region, exhibits rotational diffusion dynamics that depend significantly on the concentration of anesthetic present in the system, and it is the results for this chromophore which are the focus of this Chapter.

Perylene has been studied in lipid bilayer structures before.^{41,48-51} Measurements on perylene in DMPC bilayers as a function of system temperature revealed the sensitivity of this

chromophore to phase transitions within the lipid acyl chain region.^{41,52} DMPC exhibits a gel-to-fluid phase transition at 24°C and, for perylene incorporated in DMPC vesicles less than *ca.* 800 nm diameter, this phase transition influences the reorientation dynamics significantly.⁴¹ For vesicles of 1 μm diameter and larger, the reorientation dynamics of perylene are no longer sensitive to the phase transition.⁴¹ This is because for small diameter vesicles the structural asymmetry between the inner and outer leaflets is sufficient to cause perylene to partition preferentially into one of the leaflets.⁴¹ For larger diameter vesicles the structural asymmetry between the inner and outer leaflets becomes negligible and the chromophore resides in the inter-leaflet gallery.⁴¹ For the work described here, perylene is used as the chromophore because of its ability to sense local organization and the vesicles are maintained at a diameter of *ca.* 400 nm in order that the chromophore will reside within one of the lipid leaflets rather than in the inter-leaflet gallery.⁴¹

Two bodies of data have been measured for perylene in vesicles composed of phospholipid, sphingolipid and cholesterol designed as a simple model of the composition of neuronal cell plasma membranes. These bodies of data are the fluorescence lifetime and fluorescence anisotropy decay of perylene in vesicles as a function of exposure to varying concentrations of three anesthetics added to the solution. The anesthetics used are pentobarbital (Figure 1.3 D), halothane (Figure 1.10) and isoflurane (Figure 1.3 B). These general anesthetics were chosen because they are representative examples with structures that differ significantly from one another. Fluorescence lifetime data for perylene may serve as an indicator of local environment, but there is no fundamental theoretical connection between the fluorescence

lifetime behavior of a comparatively large organic chromophore and its response to changes in local environment. For this reason, fluorescence lifetime data can be informative at a qualitative level, at best, for the systems reported here.

Fluorescence anisotropy decay data, however, has a well-established theoretical framework within which they can be interpreted.⁵³⁻⁵⁶ It is information from these data that are most useful in revealing the effects of general anesthetics on lipid bilayer structures. Before considering the experimental data in detail, the theoretical basis for their interpretation is presented. The operative mechanism for fluorescence anisotropy decay in the systems examined here is the rotational diffusion of the chromophore. In solution, there exists an orientationally random distribution of chromophores prior to optical excitation. Excitation of the sample with a vertically polarized pulse of light photo selects an orientationally non-random subset of all chromophores present. This nonrandom subset of chromophores re-randomizes after excitation and it is the rate(s) and manner in which this relaxation process occurs that provides insight into local restrictions on the ability of the chromophore to rotate. Such restrictions on chromophore motion reveal local organization in the system and characterizing them as a function of changes in the system (*e.g.* anesthetic concentration) provides insight into the interactions between anesthetic and lipid bilayer acyl chains.

For fluorescence anisotropy decay measurements, polarized emission transients $I_{\parallel}(t)$ and $I_{\perp}(t)$ are combined to produce the induced orientation anisotropy function, $R(t)$ (equation 2.5). It is the functional form of $R(t)$ that contains chemical information. Chuang and Eisenthal have developed the theoretical basis for relating $R(t)$ to the rotational diffusion constant of the chromophore, $D = \frac{1}{3}(D_x + D_y + D_z)$, and the relative orientations of the absorbing and emitting

transition dipole moments.⁵³ To apply the Chuang and Eisenthal theory, the Cartesian axes of the chromophore are assigned, with the axis of the absorbing transition dipole moment defining the x-axis.⁵³ For perylene, the $S_1 \leftrightarrow S_0$ transition dipole moment is oriented along the molecular long axis in the plane of the π system. For the discussion that follows, the y-axis for perylene is the short in-plane axis and z is perpendicular to the chromophore π system plane.

For a spherical rotor, where the Cartesian components of the rotational diffusion constant are all equal, the anisotropy decay time is related directly to D through the Debye-Stokes-Einstein equation⁵⁴⁻⁵⁶,

$$\tau_{OR} = 6D^{-1} = \frac{\eta V}{k_B T} \quad (3.1)$$

Where η is the viscosity of the surrounding medium, V is the volume of the chromophore (for perylene $V = 225 \text{ \AA}^3$)⁵⁷, k_B is the Boltzmann constant the T is the temperature. It is the rare exception for chromophores to sweep out a spherically symmetric volume as they rotate. In situations where the Cartesian components of D, are unequal, two model cases can provide insight into the motional properties of the chromophore. Specifically, when $D_x > D_y = D_z$, the chromophore is termed a prolate rotor, and for $D_z > D_x = D_y$ the chromophore is termed an oblate rotor. From Chuang and Eisenthal's work,⁵³ for x-polarized absorbing and emitting transitions, a prolate rotor (Figure 3.2 C) will decay as

$$R(t) = 0.4 \exp(-6D_z t) \quad (3.2)$$

and an oblate rotor (Figure 3.2 B) will decay as

$$R(t) = 0.1 \exp(-(2D_x + 4D_z)t) + 0.3 \exp(-6D_x t) \quad (3.3)$$

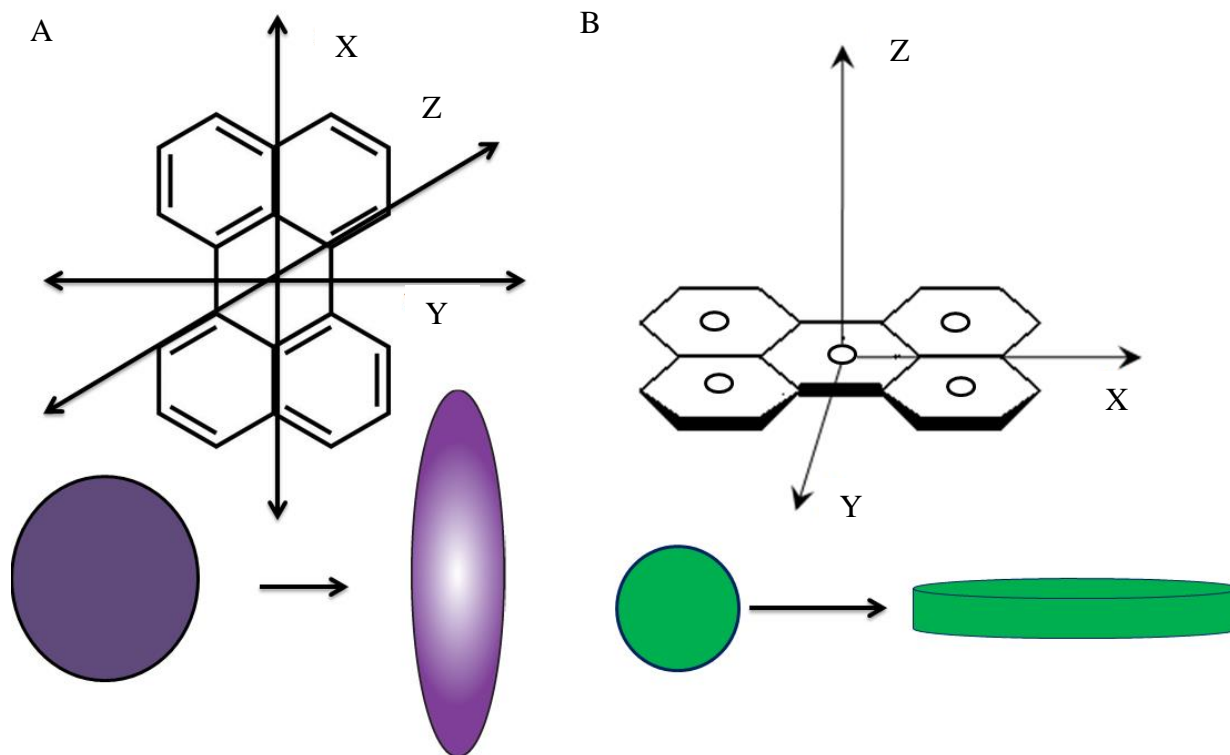


Figure 3.2: A. How perylene would orientate in the Cartesian components if it were a prolate rotor B. How perylene would orientate in the Cartesian components if it were an oblate rotor

Thus, the number of exponential decays contained in $R(t)$ is determined by the asymmetric nature of the chromophore rotational motion. For the measurements reported in this work, two-component anisotropy decay is seen in all cases. From the experimental data and the use of Equation 3.4, it is possible to extract D_x and D_z , and from the definition of an oblate rotor (*vide infra*), $D_x = D_y$, allowing D to be determined.

Experimentally, two time constants are recovered from the anisotropy decay data. These time constants are related to D_x and D_z according to Equation 3.4 and 3.5⁵³,

$$D_x = \frac{1}{6\tau_{slow}} \quad (3.4)$$

$$D_z = \frac{1}{4} \left(\frac{1}{\tau_{fast}} - \frac{1}{3\tau_{slow}} \right) \quad (3.5)$$

The quantities of interest are the values of $D_x (=D_y)$ and D_z , and the ratio D_z/D_x as a function of anesthetic concentration. We present these data in Tables 3.1 and 3.2, and in Figures 3.3 through 3.6. The time constants in Table 3.1 were extracted from experimental data. What can be observed from the data tabulated data in 3.1 is that there is not a dose dependency trend in the data set. For the fluorescence lifetime measurements the data were fitted to the function $f_{fl}(t)=I_0exp(-t/\tau_{fl})$ and for the anisotropy decay measurements the data were fitted to the function $f_R(t)=R_1(0)exp(-t/\tau_{OR1}) + R_2(0)exp(-t/\tau_{OR2})$.^{41,45,46,53} Since there is no obvious dose dependent trend in the data it is vital to break the data up into the Cartesian components of D_x , D_y , and D_z . In Table 3.2, the quantities D_x , D_y , D_z/D_x , τ_{DSE} and η_{DSE} were derived from the experimental time constants shown in Table 3.1 and Equations 3.1 and 3.3 – 3.5.

	Concentration (mM)	τ_{fl} (ps)	τ_{OR1} (ps)	τ_{OR2} (ps)
Control	0	6904 ± 14	225 ± 93	1349 ± 107
	Pentobarbital	1	6705 ± 18	63 ± 30
	2	6741 ± 19	40 ± 6	1423 ± 77
	5	7011 ± 20	57 ± 17	976 ± 54
	7	6672 ± 17	99 ± 41	1106 ± 59
	10	6960 ± 17	58 ± 25	924 ± 56
Isoflurane	2	6913 ± 17	107 ± 25	1216 ± 75
	3	6967 ± 19	145 ± 31	1339 ± 115
	5	7380 ± 21	58 ± 17	814 ± 71
	7	7159 ± 18	93 ± 19	1293 ± 95
	10	6872 ± 18	80 ± 15	1280 ± 63
Halothane	2	5977 ± 9	116 ± 27	2246 ± 70
	3	5241 ± 10	70 ± 28	2369 ± 68
	5	7128 ± 21	102 ± 35	1115 ± 92
	7	7178 ± 21	77 ± 18	1010 ± 91
	10	5112 ± 16	51 ± 14	1916 ± 97

Table 3.1: Fluorescence lifetime and anisotropy decay time constants as a function of anesthetic concentration. The fluorescence lifetime data were fitted to a single exponential decay function and the anisotropy decay data were fitted to a two-exponential decay component function.

	Concentration (mM)	D_z (MHz)	D_x (MHz)	D_z/D_x	τ_{DSE} (ps)	η_{DSE} (cP)
Control	0	1050 ± 330	124 ± 10	8.5 ± 3	385	7.1
Pentobarbital	1	3910 ± 1280	117 ± 5	34 ± 12	120	2.2
	2	6190 ± 820	117 ± 7	53 ± 10	77	1.4
	5	4300 ± 1010	171 ± 10	25 ± 7	108	2.0
	7	2450 ± 740	151 ± 8	16 ± 5	182	3.3
	10	4220 ± 1300	180 ± 12	23 ± 8	109	2.0
Isoflurane	2	2270 ± 450	137 ± 9	17 ± 4	197	3.6
	3	1660 ± 310	124 ± 12	13 ± 3	262	4.8
	5	4210 ± 990	205 ± 19	21 ± 7	108	2.0
	7	2620 ± 460	129 ± 10	20 ± 4	173	3.2
	10	3060 ± 500	130 ± 7	24 ± 5	151	2.8
Halothane	2	2120 ± 410	74 ± 2	29 ± 7	220	4.1
	3	3540 ± 1030	70 ± 3	50 ± 15	136	2.5
	5	2380 ± 640	149 ± 14	16 ± 5	187	3.4
	7	3160 ± 620	165 ± 16	19 ± 5	143	2.6
	10	4860 ± 1060	87 ± 5	56 ± 15	99	1.8

Table 3.2: D_z , D_x , D_z/D_x , τ_{DSE} and η_{DSE} values derived from experimental data as a function of anesthetic concentration.

The data contained in Table 3.2 provide significant insight into the interactions of the three anesthetics and the lipid bilayer. Before examining these details, however, it is instructive to compare the calculated viscosity values for perylene reorientation in the bilayer structures as a function of anesthetic identity and concentration (Figure 3.3). These data demonstrate three important points. The first is that all of the anesthetics are interacting significantly with the acyl chain region of the lipid bilayers which can be supported by the decrease in the viscosity of the acyl chain region in these vesicles that were treated versus those that were not. The second point of interest is that the viscosities are on the order of half what is measured for the same bilayer that has not been exposed to anesthetics. This finding is consistent with a number of other

studies on lipid bilayer structures where the addition of constituents to the lipid bilayer typically reduces the organization and thus the viscosity of the bilayer structure. The third point is that there is a slight, qualitative trend in the data toward lower viscosities with increasing anesthetic concentration *vide infra*. Again, this is not a surprising result and it is indicative of the amount of anesthetic interacting with the bilayer being proportional to the amount of anesthetic in solution. These viscosity changes are supported when the Cartesian components of perylene are analyzed.

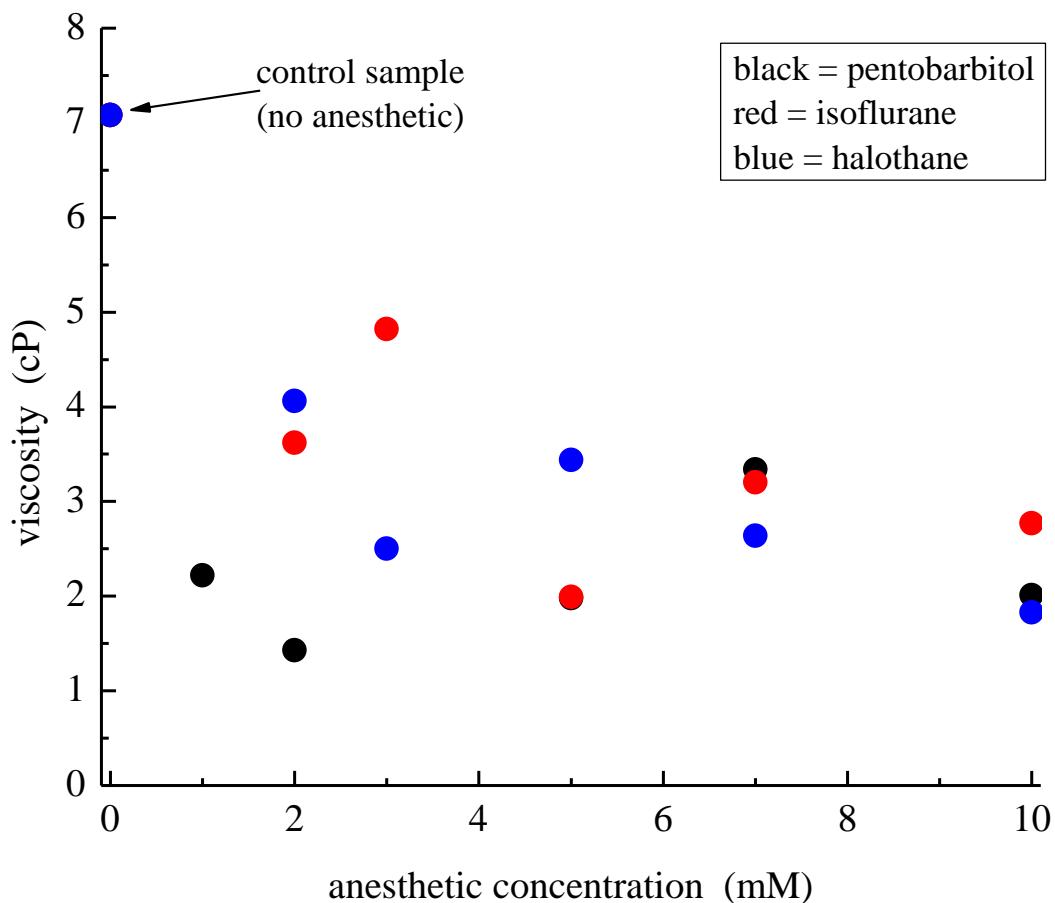


Figure 3.3. Dependence of lipid bilayer acyl chain region viscosity detected by rotational diffusion measurements and calculated using Eq. 3.1, on the identity and concentration of anesthetic present in the vesicle containing solution. Uncertainty in each data point is ± 0.5 cP.

It is clear from the data contained in Fig. 3.3 that the anesthetics are interacting with the acyl chain region of the lipid bilayer structure. With that information in hand, the anesthetic identity- and concentration-dependent values of D_x , D_z and D_z/D_x can be considered. These data are presented in Figs. 3.4 – 3.6.

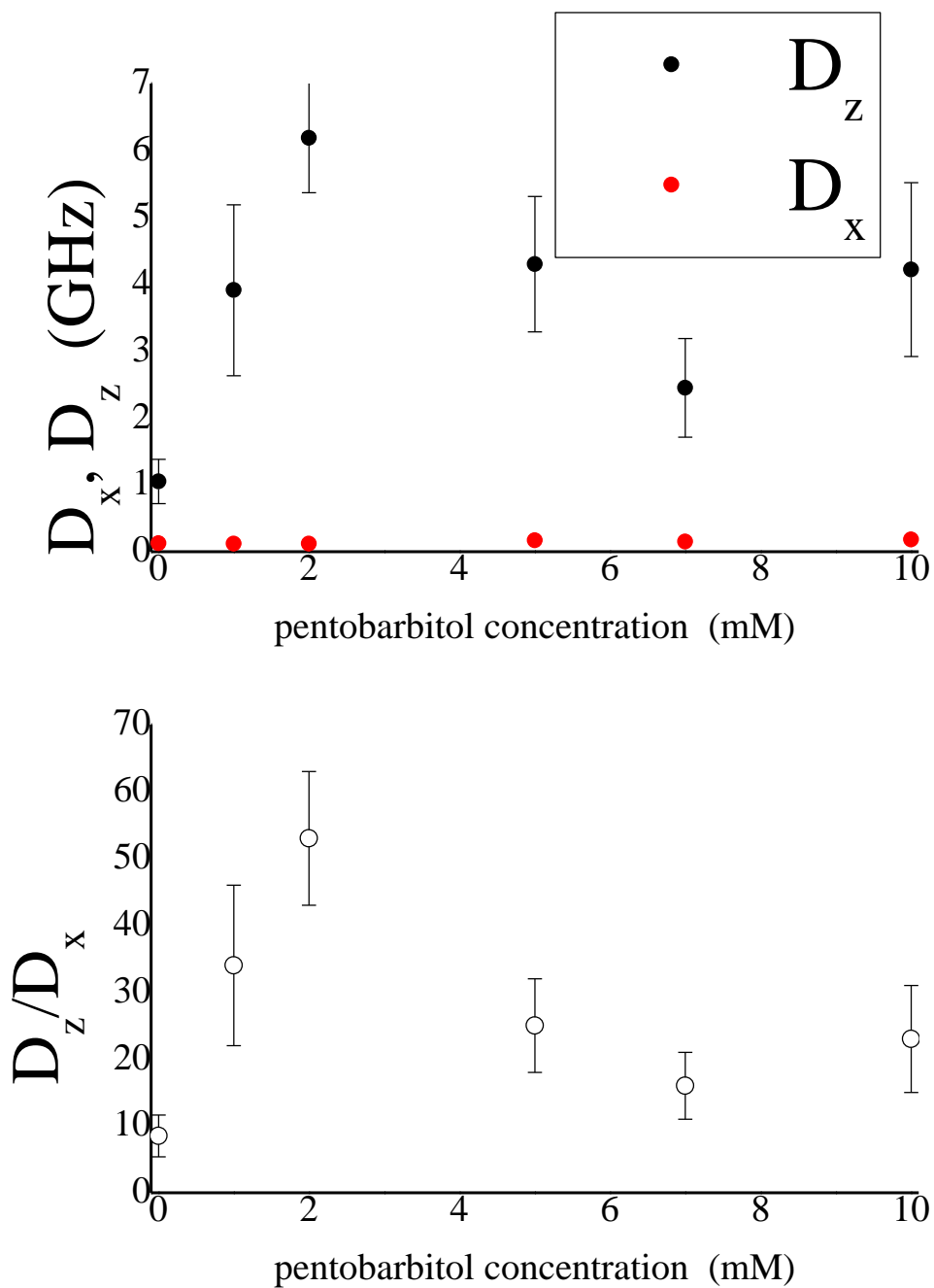


Figure 3.4. Top: D_z and D_x (GHz) as a function of pentobarbital concentration. Bottom: D_z/D_x as a function of pentobarbital concentration.

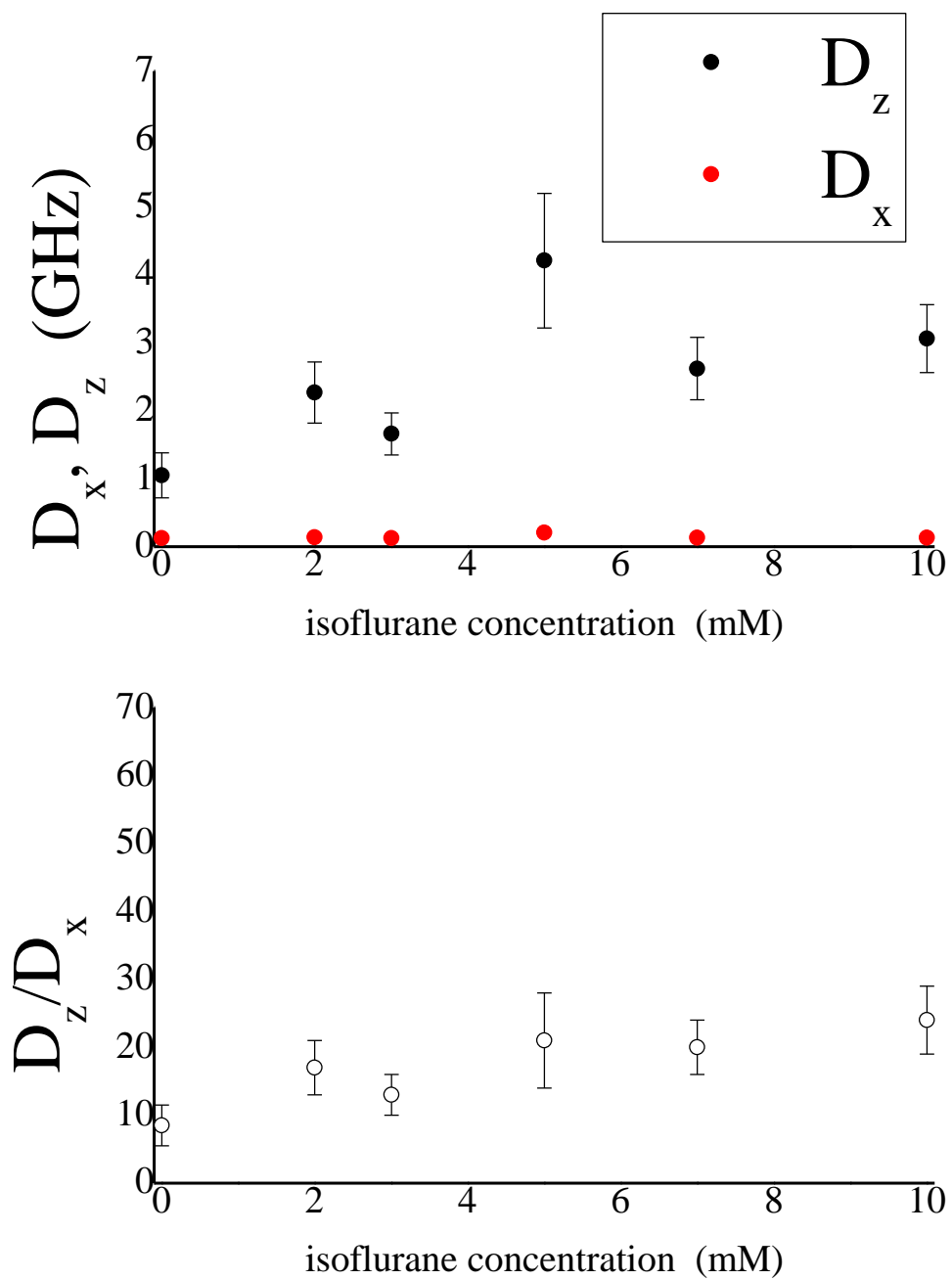


Figure 3.5. Top: D_z and D_x (GHz) as a function of isoflurane concentration. Bottom: D_z/D_x as a function of isoflurane concentration.

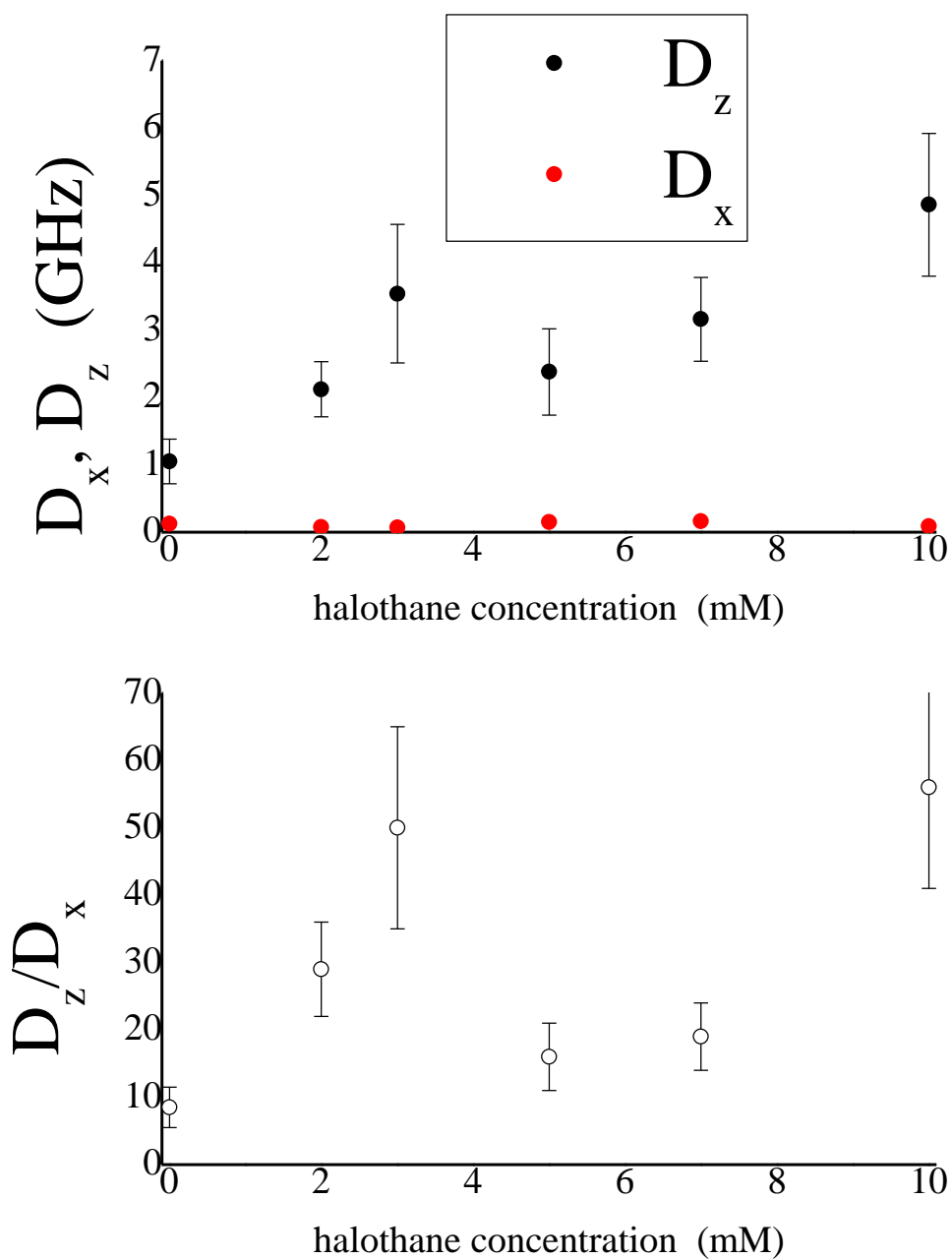


Figure 3.6. Top: D_z and D_x (GHz) as a function of halothane concentration. Bottom: D_z/D_x as a function of halothane concentration.

For all data sets, the addition of anesthetic increases the ratio D_z/D_x relative to that of the control data. This finding, in conjunction with the data in Figure 3.3 pointing to a lower local viscosity experienced by the chromophore when anesthetic is present implies that the increase in D_z/D_x does not represent a restriction of the chromophore local environment about x-axis rotation. Rather, these data imply the increased facilitation of rotational motion about the z-axis as a function of added anesthetic. Thus the addition of anesthetic to the lipid bilayer is consistent with a reduction in the order of the acyl chain region.

The data presented in Figures 3.4 – 3.6 also demonstrate an apparent discontinuity in the region between *ca.* 3 and *ca.* 5 mM anesthetic. The functional forms of these data are reminiscent of data seen for perylene reorienting in DMPC lipid bilayers at a series of temperatures, above and below the gel-to-fluid phase transition.⁴¹ The implication of such changes in D_z/D_x as a function of anesthetic concentration is that the anesthetic is interacting with the lipid acyl chain region in such a way as to alter its organization. It is noteworthy that the apparent change in lipid acyl chain organization occurs in the same concentration region for all of the anesthetics examined. While there is not a currently accepted structure-function relationship for the operation of anesthetics on bilayers, it appears that the function sensed by perylene reorientation is remarkably similar for the three anesthetics examined, despite the substantial structural differences between them.

The issue in question in this work is whether or not the action of anesthetics on lipid bilayers is related to the ability of these compounds to induce characteristic anesthetic effects. The primary issue is whether anesthetics interact with the bilayer directly or with transmembrane species to produce the desired effect. In either case, the putative mode of action is the reversible

loss of neuronal cell function. The work presented here demonstrates interactions between the lipid bilayer and the anesthetics that appear to be remarkably similar despite the structural variation of the anesthetics, this is supported with the data that indicates the increase in acyl chain viscosity. The viscosity change upon exposure to all anesthetics shows that in all cases the anesthetics are interacting with the bilayers. The data that reveal the similarities between all three are the figures showing D_z , D_x and D_z/D_x with breaks in behavior in the 0.3 – 0.4 mM concentration range in all cases. These interactions are either directly responsible for the mediating control over bilayer porosity or they alter bilayer-protein interactions which, in turn, mediate transmembrane channel activity. In either scenario, it is the anesthetic-bilayer interactions that are central to the operation of the anesthetic.

CHAPTER 4

Conclusions

We have used fluorescence anisotropy decay measurements to interrogate the local environment of lipid vesicle structures with composition intended to mimic the neuronal membrane. We have found that the acyl chain region of these vesicles undergo a measurable change in organization when exposed to varying concentrations of selected general anesthetic agents. Our findings are consistent with Modern Lipid Hypothesis (1997) that anesthetics interact with the lipid membrane. However we cannot make a claim about whether or not they interact with transmembrane proteins imbedded within the membrane since proteins were not incorporated in the membrane in this study. This finding does not exclude the possibility that the anesthetics may also act on transmembrane proteins. Interactions between anesthetics and the plasma membrane gives rise to structural changes in the membrane that lead to increased motional freedom for a chromophore imbedded within the membrane acyl chain region. This change in structure implies increased disorder in the lipid acyl chain region, a factor that may have a significant effect on the ability of transmembrane proteins to fold into their functional forms. Any resulting changes in the function of transmembrane proteins in the membrane due to induced changes in the membrane from anesthetic interactions may account for data suggesting increased or decreased neurotransmitter release upon anesthetic administration in model organisms. There remains, however, much to be learned about the mode of anesthetic action in the CNS, but this body of data has provided some insight into the molecular-scale interactions between anesthetics and lipid bilayer structures. Future work will explore further the relationship, or absence of one, between anesthetic structure and lipid bilayer structural changes,

more biorelevant concentrations of anesthetics, and subsequently, the interactions between anesthetics and transmembrane proteins.

LITERATURE CITED

LITERATURE CITED

1. Roan, S. In *CHP/PCOR News*; Los Angeles Times: Los Angeles, 2005.
2. Lagasse, R. D. *Anesthesiology* **2002**, 97.
3. Minnesota, U. O.; Academic Health Center UMN: 2012; Vol. 2012.
4. Meyer, H. H. *Arch. Exp. Pathil. Pharmacol* **1899**, 42, 109 - 118.
5. Overton, E. *Jena: Verlag von Gustav Fischer* **1901**.
6. Pohorille, A.; Wilson, M. A.; New, M. H.; Chipot, C. *Toxicology Letters* **1998**, 100 - 101, 421 - 430.
7. Contor, R. S. *Biochemistry* **1997**, 36, 2339 - 2344.
8. In *Anestheologist Newsletter*; 9 ed. 1996; Vol. 60, p 3.
9. NIH 2011.
10. Frenster, J. M.; New York, NY: Harper Collins New York, 2001.
11. Hemmings, H. C. *Anesthesiology News* **2010**, 36, 9-16.
12. In *Discoveries in Medicine* 2012; Vol. 2010.
13. Hirschfeld, S.; Hyman, H. T.; Wanger, J. J. *Archives of Internal Medicine* **1931**, 47, 259-287.
14. Wawersik, J. *J Clin Anesth* **1991**, 3, 235-244.
15. Lundy, J. S. *Proc Staff Meet Mayo Clinic* **1935**, 10, 536 - 543.
16. Pratt, T. W.; Tatum, A. L.; Hathaway, H. R.; Waters, R. M. *American Journal of Surgery* **1936**, 31, 464-466.
17. Miller, K. W.; Pang, K. Y. Y. *Nature* **1976**, 263, 253 - 255.
18. Franks, N. P.; Lieb, W. R. *Nature* **1984**, 310, 599-601.
19. Franks, N. P.; Lieb, W. R. *Nature* **1994**, 367, 607 - 614.
20. Meyer, K. H. *Trans. Farad. Soc.* **1937**, 33, 1062 - 1068.
21. Koblin, D. D. In *Anesthesia*; Miller, R., Ed.; Churchill Livingstone: New York, 1990, p 51 - 83.

22. Miller, K. W.; Paton, W. D. M.; Smith, R. A.; Smith, E. B. *Molecular Pharmacology* **1973**, *9*, 131 - 143.
23. Metcalfe, J. C.; Seeman, P.; Burgen, A. S. V. *Molecular Pharmacology* **1968**, *4*, 87 - 95.
24. Lawrence, D. K.; Gill, E. W. *Molecular Pharmacology* **1975**, *11*, 280 - 286.
25. Boggs, J. M.; Yoong, T.; Hsia, J. C. *Molecular Pharmacology* **1975**, *12*, 127 - 135.
26. Hale, J.; Keegan, R.; Smith, E. B.; Snape, T. J. *Biochimica et Biophysica Acta (BBA) - Biomembranes* **1972**, *288*, 107-113.
27. Levitt, J. D. *Anesthesiology* **1975**, *42*, 267-274.
28. Rosenberg, P. H.; Eibl, H.; Stier, A. *Molecular Pharmacology* **1975**, *11*, 879 - 882.
29. Gordesky, S. E.; Marinetti, G. V. *Biochemical and Biophysical Research Communications* **1973**, *50*, 1027-1031.
30. Weir, C. J. *Continuing Education in Anesthesia, Critical Care, and Pain* **2006**, *6*, 49 - 53.
31. Eger, E. I.; Koblin, D. D.; Harris, R. A.; Kendig, J. J.; Pohorille, A.; Halsey, M. J.; Trudell, J. R. *Anesthesia and Analgesia* **1997**, *84*, 915 - 918.
32. Pringle, M. J.; Brown, K. B.; Miller, K. W. *Molecular Pharmacology* **1980**, *19*, 49 - 55.
33. Franks, N. P.; Lieb, W. R. *Nature* **1982**, *300*, 487 - 493.
34. Hirota, K.; Sasaki, R.; Roth, S. H.; Yamazaki, M. *Anesthesia and Analgesia* **2010**, *110*, 1607-1613.
35. Ogawa, S. K.; Tanaka, E.; Shin, M. C.; Kotani, N.; Akaike, N. *Neuropharmacology* **2011**, *60*, 701-710.
36. Turina, D.; Bjornstrom, K.; Sundqvist, T.; Eintrei, C. *Journal of Physiology and Pharmacology* **2011**, *62*, 119-124.
37. Nelson, S. C.; Neeley, S. K.; Melonakos, E. D.; Bell, J. D.; Busath, D. D. *BMC Biophysics* **2012**, *5*, 5.
38. Pillman, H. A.; Blanchard, G. J. *Journal of Physical Chemistry B* **2010**, *114*, 3840 - 3846.
39. Botchway, S.; Lewis, A.; Stubbs, C. *European Biophysics Journal* **2011**, *40*, 131-141.
40. Skoog, D. A.; Holler, F. J.; Crouch, S. R. In *Instrumental Analysis*; Brooks/Cole, Ed.; Cengage Learning: New Delhi, 2007, p 443-476.
41. Lapinski, M. M.; Blanchard, G. J. *Chemistry and Physics of Lipids* **2008**, *153*, 130-137.

42. Karpovich, D. S.; Blanchard, G. J. *Journal of Physical Chemistry* **1995**, *99*, 3951-3958.
43. Nestler, E. J.; Hyman, S. E.; Malenka, R. C. *Molecular Neuropharmacology: A Foundation for Clinical Neuroscience*; McGraw Hill: New York, 2009.
44. *Fundamentals of Anesthesia*; 3 ed.; Cambridge University Press: Cambridge, 2009.
45. Dewitt, L.; Blanchard, G. J.; LeGoff, E.; Benz, M. E.; Liao, J. H.; Kanatzidis, M. G. *Journal of the American Chemical Society* **1993**, *115*, 12158.
46. Delacruz, J. L.; Blanchard, G. J. *Journal of Physical Chemistry B* **2003**, *107*, 7102.
47. Pillman, H. A., Michigan State University, 2010.
48. Christensen, R. L.; Drake, R. C.; Phillips, D. *Journal of Physical Chemistry* **1986**, *90*, 5094-5097.
49. Klein, U. K. A.; Haar, H. P. *Chemical Physics Letters* **1979**, *63*, 40-42.
50. Labhart, H.; Pantke, E. R. *Chemical Physics Letters* **1990**, *23*, 482-485.
51. Zinsli, P. E. *Chem Phys* **1977**, *20*, 299-309.
52. Koan, M. M.; Blanchard, G. J. *Journal of Physical Chemistry B* **2006**, *110*, 16584-16590.
53. Chuang, T. J.; Eisenthal, K. B. *J. Chem. Phys.* **1972**, *57*, 5094-5097.
54. Debye, P. *Polar Molecules*; New York: New York, 1929.
55. Perrin, F. *J. Phys. Radium* **1936**, *7*, 1-11.
56. Zwanzig, R.; Harrison, A. K. *Journal of Chemical Physics* **1985**, *83*, 5861-5862.
57. Edward, J. T. *Journal of Chemical Education* **1970**, *47*, 261-270.